Check for updates

*CORRESPONDENCE
Adline Princy Solomon
✉ adlineprinzy@sastra.ac.in
Helma David
✉ helmadavid@scbt.sastra.ac.in

†These authors have contributed equally to
this work

Aptamers: precision tools for diagnosing and treating infectious diseases

Swathi Sujith[†], Rajalakshmi Naresh[†], B. U. Srivisanth[†],
Anusree Sajeevan, Shobana Rajaramon, Helma David*
and Adline Princy Solomon*

Quorum Sensing Laboratory, Centre for Research in Infectious Diseases (CRID), School of Chemical
and Biotechnology, SASTRA Deemed to be University, Thanjavur, India

Infectious diseases represent a significant global health challenge, with bacteria, fungi, viruses, and parasitic protozoa being significant causative agents. The shared symptoms among diseases and the emergence of new pathogen variations make diagnosis and treatment complex. Conventional diagnostic methods are laborious and intricate, underscoring the need for rapid, accurate techniques. Aptamer-based technologies offer a promising solution, as they are cost-effective, sensitive, specific, and convenient for molecular disease diagnosis. Aptamers, which are single-stranded RNA or DNA sequences, serve as nucleotide equivalents of monoclonal antibodies, displaying high specificity and affinity for target molecules. They are structurally robust, allowing for long-term storage without substantial activity loss. Aptamers find applications in diverse fields such as drug screening, material science, and environmental monitoring. In biomedicine, they are extensively studied for biomarker detection, diagnostics, imaging, and targeted therapy. This comprehensive review focuses on the utility of aptamers in managing infectious diseases, particularly in the realms of diagnostics and therapeutics.

1 Introduction

Pathogens, such as bacteria, fungi, viruses, or parasitic protozoa transmitted throughout populations, are typically the source of infectious diseases, some recognized as potentially fatal (Wan et al., 2021; Krüger et al., 2021; Zhang et al., 2021). Infectious diseases continue to be a significant global public health concern, representing the primary causes of morbidity and mortality (Cohen, 2000). Similar signs and symptoms are common among numerous diseases, and the diagnosis, treatment, and management of infectious diseases may face significant difficulties due to the emergence of novel pathogens as well as the reappearance and rise of previously identified pathogen variations (Chen et al., 2022b)

(Wan et al., 2021). The rise of antimicrobial resistance can be attributed to the improper or empirical use of antibiotics in the treatment of infections. This underscores the need for careful and evidence-based antibiotic management in addressing infectious diseases (Fair and Tor, 2014; Rahbi et al., 2023). While laboratory testing, imaging scans, and biopsies based on clinical signs and epidemiological data have been successfully used to identify infections, these conventional procedures are either labor-intensive or highly complex (Wan et al., 2021; Zhang et al., 2021).

Therefore, it is imperative to develop new, quick, and precise diagnostic and therapeutic techniques to address the issues of drug resistance and anti-microbial resistance (Krüger et al., 2021). Aptamer-based diagnostic technologies are among the diagnostic approaches that are rapidly being employed for molecular disease diagnosis due to their cost-effectiveness, sensitivity, specificity, and convenience (Wan et al., 2021). The Latin word "aptus", which means "to fit," and the Greek word "meros", which means "region," are the sources of the word "aptamer" (Ku et al., 2015). Aptamers, single-stranded RNA or DNA oligonucleotide sequences with a length of approximately 25–80 bases, are the nucleotide counterparts of monoclonal antibodies. They may bind target molecules with high affinity and specificity, demonstrating the nucleic acid's multifunctional nature (Ni et al., 2021). Aptamers offer a range of benefits, such as being cost-effective, exhibiting minimal batch-to-batch variation, demonstrating low immunogenicity, and possessing a small size for improved tissue penetration (Otte et al., 2022). Despite their potential, aptamers are constrained by their rapid clearance through renal filtration and susceptibility to nuclease hydrolysis, leading to a very short half-life *in vivo* (Kovacevic et al., 2018; Ni et al., 2021). In response to these limitations, several techniques have been developed to extend the half-life. These include PEGylation for sustained action, modification of sugar ring or base, phosphodiester linkage, and 3′ end capping with inverted thymidine (Ni et al., 2017). Due to their structural stability, aptamers can be manufactured in large quantities and stored for extended periods without significant activity loss (Srivastava et al., 2021).

Various aptamers have been developed against various targets such as hormones, viruses, metal ions, proteins, viruses, and bacteria (Zhou and Rossi, 2017; Shraim et al., 2022). These complexes form stable and specific targets with dissociation constants in the nanomolar range. Additionally, aptamers have a greater target range, it is easier to regenerate, substantially smaller, and is neither poisonous nor immunogenic (García-Recio et al., 2016; Zheng et al., 2015; Roxo et al., 2019). New aptamer reports are released nearly daily due to their broad applicability. A specific database has been built (https://sites.utexas.edu/aptamerdatabase) to classify the aptamer-related data and enable access to information about various existent aptamers (Askari et al., 2024). Aptamers have drawn a lot of interest in the biomedical community due to their unique qualities and wide applications in a variety of sectors, including drug screening, material science, and environmental monitoring (Chen et al., 2022a).

Aptamers have been extensively studied and developed over the past 20 years by researchers in several biomedical fields, including biomarker detection, diagnostics, imaging, and targeted therapy.

Aptamers that are now utilized in cancer treatment can bind to and block the immunoregulatory components of carcinogenesis, which are particular to molecular targets that are characteristic of various diseases. In December 2004, the US Food and Drug Administration approved pegaptanib (Macugen), the first medication based on aptamer technology, for the treatment of age-related macular degeneration (Adachi and Nakamura, 2019). Despite the lack of new aptamers approved for clinical use, there is promising progress in the development of aptamers for blood disorders, with several of them currently undergoing different stages of clinical trials and proof-of-concept investigations (Aljohani et al., 2022). Aptamers demonstrate a wide range of applications, highlighting their versatile nature in the field of infectious diseases. Thus, the review provides an in-depth insight into the general mechanism of aptamer selection and its applications in the diagnostic and therapeutic fields. Furthermore, it addresses recent advances and challenges in the field of aptamers, aiming to inspire further exploration of aptamer-based approaches in combating infectious diseases.

2 Mechanisms of aptamer selection

The process of aptamer selection includes a range of methodologies designed to identify nucleic acid sequences that can bind specific target molecules with high affinity and specificity (Kinghorn et al., 2017). Both SELEX (Systematic Evolution of Ligands by Exponential Enrichment) and non-SELEX approaches are used to refine methods. SELEX employs iterative rounds of selection, in which a nucleic acid library interacts with the target molecule under controlled conditions, to enhance sequences with optimal binding properties (Uemachi et al., 2021). Contrastingly, Non-SELEX methods steer clear of traditional scaffold-based approaches, opting instead for innovative strategies to bolster aptamer stability, specificity, and interaction dynamics (Kong and Byun, 2013). These diverse methodologies empower researchers to confidently tailor aptamer selection processes according to the specific requirements of their applications, from diagnostics to therapeutic interventions.

2.1 Systematic evolution of ligands by exponential enrichment

SELEX is a method used to derive aptamers from a pool of nucleotide sequences that exhibit high affinity and selectivity (Chen et al., 2016). The process involves several key steps to select aptamers through a repetitive cycle of amplification and enrichment. Initially, a large and diverse library of nucleic acid sequences (DNA or RNA) is synthesized and incubated with the target molecule in an appropriate buffer at a specific temperature (Sun et al., 2014). The partitioning or the eluting steps involves removal of the unbound nucleotide by chromatography, electrophoresis or filtration (Dong et al., 2018). A low ratio of nucleic acid sequences to the target molecule is used, ensuring effective binding. The aptamer-target complexes are then separated from unbound sequences using techniques such as capillary

electrophoresis (Hamedani and Müller, 2016), magnetic bead separation (Yüce et al., 2015), and flow cell methodologies (Gopinath, 2007).

The bound sequences are eluted from the target and amplified using PCR for DNA aptamers or reverse transcription followed by PCR for RNA aptamers, creating a new, enriched library. These processes are repeated for several rounds, typically 8-15, to enhance the prevalence of high-affinity species, which eventually dominate the library (Zhou and Rossi, 2017) (Figure 1). After multiple rounds of selection, the enriched library is cloned and sequenced to identify individual aptamer sequences, which are then validated for their binding performance. Through these iterative rounds, SELEX effectively isolates aptamers that can bind to specific target molecules with high affinity and specificity. However, a common drawback of aptamers derived from traditional SELEX methods is poor or nonspecific detection performance in diagnostic applications (Bakhtiari et al., 2021). To overcome these shortfalls, different methodologies are incorporated over conventional SELEX, some of which are discussed below.

2.1.1 Magnetic beads SELEX

Magnetic SELEX is a method that is commonly employed as this method offers ease in the separation of the target and nucleotide sequence easily from the remaining reaction mixture by employing a magnet (Yüce et al., 2015). When the DNA sequence binds with the target molecule, the mixture is now added with magnetic beads coated with a molecule that can selectively bind with the nucleic acid sequence attached to the target molecule. The elution of the bound nucleic acid sequences from the magnetic beads is achieved by altering the buffer's properties, applying heat, or utilizing other methods that hinder the nucleic acids' binding to the magnetic beads (Komarova and Kuznetsov, 2019). In previous research, the isolation of Metamitron (MTM) aptamers using magnetic-bead SELEX has been successful. MTM, a widely used herbicide in agriculture, has been the subject of a thorough investigation. It is important to note that even with significant exposure, the negative health effects on humans are minimal. Following ten rounds of screening, high-throughput sequencing successfully identified six

FIGURE 1

Illustration of SELEX strategies for aptamer synthesis. (1) The process begins with the preparation of a nucleotide pool, which is then incubated with target cells. (2) Various SELEX methods, such as Capillary Electrophoresis SELEX, SPR-SELEX, Whole Cell SELEX, and Magnetic Beads SELEX, are employed to facilitate the selection of aptamer-target complexes. (3) & (4) These complexes are isolated, and the bound aptamers are subsequently amplified by PCR. (5) The cycle is repeated multiple times to enhance the specificity and affinity of the aptamers for their targets. Created using Biorender.com.

outstanding candidate aptamers with remarkable affinity and specificity (Xie et al., 2022).

2.1.2 Capillary electrophoresis

Apart from using traditional gel electrophoresis, capillary electrophoresis (CE) is employed to derive aptamer candidates on the metrics of sizes and charge; under the electric field, capillary electrophoresis can separate molecules as tiny as porphyrin30 (Yüce et al., 2015). When performing CE-SELEX, the target molecules are subjected to incubation with the random library in free solution, and the resulting combination of free target molecules, target-ssDNA complexes, and free ssDNA is then fed into a capillary column, then split apart using a high voltage. Taking a sample of the output fraction at the designated retention time, target-bond ssDNA provides the chance to collect DNA aptamers that bind to a specific target (Hamedani and Müller, 2016). Demonstrating the perspective of CE-SELEX for small-molecule targets in just four rounds. Small-molecule targets are anticipated to alter the mobility of the complex only slightly from the nonbinding sequences, leading to only partial separation of the bound and unbound sequences. However, even if just a tiny amount of the complex can be recovered, adequate enrichment can be accomplished since nucleic acids can be exponentially amplified by polymerase chain reaction (PCR). Additionally, repeated recurrent rounds of enrichment can eventually lead to the evolution of an abundant pool with high quality, even in the situation of separation with poor resolution (Yang and Bowser, 2013).

When CE-SELEX and high throughput sequencing (HTS) gave higher efficiency with faster separation of target-ssDNA complex and free ssDNA in free solution, aptamers can be chosen with relatively fewer rounds of selection thanks to HTS, which offers insight into the sequence evolution during the CE-SELEX process and makes it possible to characterize the entire evolutionary path. This reduces the need for the pool to occupy a consensus sequence and increases selection efficiency (Zhu et al., 2021).

2.1.3 Whole cell SELEX

While the major targets for the other SELEX techniques are highly purified targets, whole cell-SELEX uses a complete cell as the target. The cell-SELEX procedure may aim for extracellular cell surface proteins or unidentified cell structures. This SELEX approach makes it possible to create whole-cell targeting aptamers without much prior information on the cell's surface proteins, which facilitates the identification of new biomarkers primarily for diagnosis and imaging (Yüce et al., 2015). The whole-cell SELEX method is used to create highly selective aptamers by different rounds of SELEX and counter SELEX. Aptamer can be separated using methods such as flow cytometry, Magnetic-Activated Cell Sorting, Differential Centrifugation, and Label-free methods. Whole-cell SELEX yields aptamers with high affinity and specificity when targeting bacterial surface compounds and live bacterial cells. Flow cytometry is a vital method for identifying target aptamers that bind selectively to cells. The technique overcomes the limitations of whole-cell SELEX by sorting, counting, and detecting fluorescence (Moon et al., 2013).

Within flow cytometry techniques, fluorescence-Activated Cell Sorting (FACS) technique offers the ability to simultaneously differentiate and separate cell subpopulations, facilitating the identification of bound and unbound aptamers with specificity along with isolation of functional nucleic acids. By utilizing a sorting device that efficiently separates specific cells based on their fluorescence, FACS streamlines the process of finding aptamers that target different cell types contributing to a better yield of the aptamer candidates. The effectiveness of FACS in SELEX for functional aptamer selection is apparent in its successful separation of *E. coli* cells that produce RNA mimics (Nishimoto et al., 2007; Mayer et al., 2010; Zou et al., 2015). FACS is an effective method for large-scale aptamer screening because it is a fast and accurate technique that can process thousands of cells per second. It can sort cells based on multiple parameters and select aptamers based on their binding to live cells or complex mixtures, which may be more representative of physiological conditions than selections made *in vitro*. The possibility of obtaining high-quality aptamers is increased by the capacity to sort and enrich high-affinity binders from a huge library. FACS employs both positive and negative selection strategy, thereby reducing the experimental steps and experimental errors in the cell SELEX process, hence saves times. DNA Aptamers against Burkitt's lymphoma cells which exhibit a characteristic phenotype was chosen using positive selection methods (Ohuchi, 2012; Raddatz et al., 2008; Sola et al., 2020). Despite the benefits of the cell-SELEX system, the low aptamer enrichment performance of this technique is caused by the co-expression of several off-target surface indicators and compounds on the target cells (Sun et al., 2014).

2.1.4 Surface plasmon resonance or flow cell SELEX

SPR- SELEX utilizes SPR for the selection process, differentiating it from the other methods. A Randomized library is passed over a surface coated (gold surface) with the target molecule (Yüce et al., 2015). In the library, a diverse range of oligonucleotides interact with the target in various ways. Oligonucleotides demonstrating strong binding will firmly adhere to the target-coated surface, while those with weak binding or unbound sequences will be effectively washed away (Jia et al., 2018). In SPR the nucleic acid sequence bound to the target molecule will be monitored in real time by observing the change in the refractive index on the surface leading to the change in surface plasmon signal (Ferhan et al., 2016). With the help of the above-mentioned steps, specific aptamer candidates are carefully selected and amplified using PCR (Jia et al., 2018).

2.2 Non-SELEX methods

SELEX uses a nucleic acid scaffold to develop the aptamer; however, other techniques do not require scaffolds (Reverdatto et al., 2015). For instance, aptamers are produced in the RNase III-deficient *E. coli* HT115(DE3), and 5′- and 3′ ends of the RNA transcript are protected from the RNase using double stranded

spacers. This method only required fewer nucleotides than scaffold-based methods like the other different types of SELEX used to avoid RNase activity on the formed aptamer (Zou et al., 2023). PhotoSELEX, featuring photoreactive nucleic acids, confidently enhances control over the selection process. Upon exposure to light, the photoreactive groups confidently form covalent bonds between the selected aptamers and the target molecule, confidently providing a reliable method for identifying and capturing aptamer-target complexes (Brody et al., 1999). Graphene oxide (GO) is composed of carbon atoms arranged in a hexagonal lattice. Its unique properties allow for the immobilization of arbitrary DNA or RNA sequences on its surface, forming an oligonucleotide library with diverse sequences. During the GO-SELEX process, the target molecule interacts with the library-immobilized sequences. In the presence of the target molecule, the immobilized sequences on the GO surface are released and precisely interact with the target. This stage allows for the selection of aptamers with a high affinity for the target molecule (Nguyen et al., 2014; Ding and Liu, 2023). In the Capture-SELEX process, a DNA library is immobilized onto a substrate. The target of interest is then passed through to extract eluted aptamers. Aptamers are specifically chosen using this strategy for solute targets (Boussebayle et al., 2019). These non-SELEX methods provide versatile alternatives, overcoming challenges such as RNase degradation, and enhancing binding affinity through innovative selection techniques.

The aptamers that are selected can be used in various applications. One groundbreaking application is the use of apta-sensors for detecting infectious diseases. These biosensors use aptamers as recognition elements, and they provide fast, sensitive, and specific detection of pathogens. By incorporating aptamers selected through SELEX or Non-SELEX methods, apta-sensors can accurately detect infectious agents, greatly improving diagnostic capabilities. Their versatility and ability to detect a wide range of pathogens make aptasensors extremely valuable tools in epidemiology, healthcare settings, and biodefense (Brosseau et al., 2023).

3 Aptamers in diagnostics of infectious diseases

Traditional methodologies for detection encompass culture-based techniques and color culture medium approaches. However, these methodologies are encumbered by limitations, necessitating professional expertise, and demanding cumbersome labor and time commitments. The procedural intricacies include pre-enrichment, selective enrichment, and biochemical identification, typically leading to a confirmed outcome after 2-3 days (Bell et al., 2016). Due to the limitations present in these methods, there is a need for more efficient, rapid and accurate diagnostic methods. Immunological assays, such as ELISA and immunosensors, are commonly used for bacterial detection. However, their sensitivity is limited because proteins like immunoglobulins cannot be amplified. Furthermore, nucleic acid-based assays are unable to distinguish between viable and non-viable cells, as DNA can persist in the environment long after cell

viability has been lost. This creates a need for a more specific, sensitive, and convenient diagnostic method that can bridge the gap between the detection. Aptamer-based assays are utilized for the detection of pathogens and biomarkers. Aptamers synthesis is rapid compared to the antibody production, and these rapid turnaround time helps in timely diagnosis. Furthermore, they have increased stability and shelf life compared to antibodies and reduced risk of immunogenicity due to ease of modifications that increase the stability, binding affinity and functionality (Ali et al., 2019). These assays enhance detection methods by providing improved specificity and sensitivity even at lower concentrations compared to traditional methods (Aslan et al., 2023). By delivering rapid results, which are ideal for point-of-care settings, this approach enhances diagnostic efficiency across various healthcare applications (Majdinasab et al., 2022). Further, the review delineates a comprehensive analysis of the diverse categories of apta-sensors. (Figure 2, Table 1).

3.1 Optical aptasensors

The components of an optical biosensor are an optical transducer system coupled with a biorecognition sensor. Optical biosensors are designed to generate a signal that is directly proportional to the concentration of the analyte (Damborský et al., 2016). Optical aptasensors are biosensors in which the biorecognition sensing element is an aptamer. The transduction method can be SPR, fluorescence, surface enhanced raman scattering (SERS) and chemiluminescence (Uniyal et al., 2023). Optical sensors are frequently used in aptasensors because of their high sensitivity, robustness, reliability, good temporal and spatial control, selectivity, simplicity, versatility, and wide linear range for biomolecule detection (Chen et al., 2021c).

3.1.1 Surface plasmon resonance based aptasensors

When a plane polarized light falls on a thin sheet of metal, plasmons (group of electrons that undergo oscillation due to energy absorption) are formed. In context of aptasensors, aptamer-functionalized metal particles are used. When the analyte binds to the aptamer, it causes changes in the refractive index at the interface, altering the resonance condition of the surface plasmons. These changes can be observed as variations in the angle or intensity of reflected light (Schasfoort, 2017). The sensitivity and selectivity of SPR-based sensors can be significantly improved by utilizing gold nanoparticles linked to ligands that are specific to the target. SPR assays are commonly used in dual-recognition biosensors and sandwich assays to enhance detection capabilities (Kim et al., 2018a).

3.1.2 Fluorescence based aptasensors

In this type of biosensing there are usually two probes involved-the capture probe that binds to the infectious agent and the signaling probe which is usually a nanoparticle that is tagged with a fluorophore. The interaction between the analyte and the
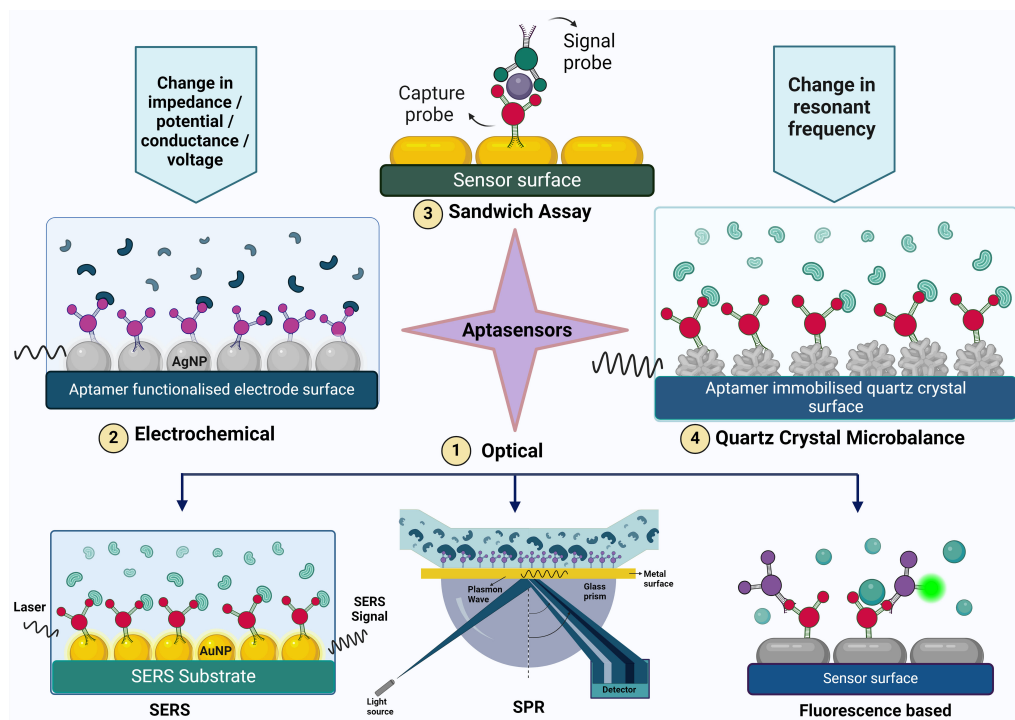
FIGURE 2
The figure illustrates various aptasensing mechanisms used for detecting target molecules. These mechanisms include (1) Optical sensors (such as Surface-Enhanced Raman Scattering (SERS), Surface Plasmon Resonance (SPR), and fluorescence-based methods), (2) Electrochemical sensors, (3) Sandwich assays, and (4) Quartz Crystal Microbalance (QCM). Each mechanism provides a unique approach to aptamer-based detection, highlighting the versatility and specificity of aptamers in biosensing applications.

aptamers leads to a rise in the fluorescence signal, which is detectable and can be analyzed in both qualitatively and quantitatively. Examples of fluorescent labels are Lanthanide-doped upconversion nanoparticles (UCNPs), silver nanoclusters (AgNCs) (Zhang et al., 2020), carbon quantum dots (CQDs) (Pebdeni et al., 2020), CdTe quantum dots and thiazole orange (Pang et al., 2015).

UCNPs have distinctive optical and chemical characteristics, including excellent photostability, low light scattering, low autofluorescence backgrounds, and low toxicity (Liu et al., 2021). AgNCs have the advantages of high quantum yield, strong photostability, low toxicity, adjustable fluorescence emission, and excellent biocompatibility (Zhang et al., 2020).

An important application of fluorescence spectroscopy is förster resonance energy transfer (FRET). It involves non-radiative transfer of energy from an excited donor fluorophore to an acceptor fluorophore that are in proximity. This phenomenon is also called quenching. Graphene oxide is a commonly used quencher molecule (Verma et al., 2023). For example, Pebdeni et al. discovered that CDQs emit blue-colored fluorescence, which is quenched in the presence of aptamers and gold nanoparticles. With the introduction of specific bacteria, the aptamer-target complex was effectively assembled, leading to the restoration of free CQD emission. The linear range of this aptasensor was 10^8 to 10^1 CFU/mL, with a detection limit as low as 10 CFU/mL for *S. aureus* (Pebdeni et al., 2020). Colorimetric aptasensors work by detecting changes in the color due to the binding of the aptamer to the analyte. This is done with the help of UV-visible spectroscopy. A peak

is obtained at a specific wavelength and stokes shift takes place (Weerathunge et al., 2019).

3.1.3 SERS based aptasensors

Surface-enhanced Raman scattering (SERS) is a phenomenon in which the Raman scattering signals are amplified by enhancing the sensor surface. Nanostructured surfaces, usually made of metals such as gold or silver, are shaped into nanoparticles, nanorods, or nanostars. These structures demonstrate strong localized surface plasmon resonance (LSPR), resulting in the enhancement of Raman signals of nearby molecules through electromagnetic and chemical mechanisms. The SERS substrates are aptamers and when the infectious agent binds to the aptamer, there is a change in the raman signal that is detected (Zhou et al., 2020).

3.1.4 Chemiluminescence based aptasensors

Chemiluminescence-based aptasensors rely on the emission of light resulting from a chemical reaction between a luminophore (a molecule capable of emitting light) and a substrate or analyte, often facilitated by enzymatic reactions (Chen et al., 2021b). A DNA aptasensor to detect norovirus GII capsid was developed based on guanine chemiluminescence detection and the principle of intra chemiluminescent resonance transfer. The high-energy intermediates formed from the reaction of extra guanines and TMPG transferred the energy to 6-FAM which caused bright chemiluminescence (Kim et al., 2018a).

TABLE 1 Pathogen detection table: Pathogens, aptamer sequences, and detection mechanisms.

S.No.	Aptamer sequence (5′ to 3′)	Type	Organism	Target	Concentration range	LOD (limit of detection)	Methodology	Reference
				Bacteria				
1.	S-S- ATCCGTCACACCTGCTCTGTCTGCGAGCGGGGC GCGGGCC CGGCGGGGGATGCGTGGTGTTGGCTCCCGTAT	DNA	E. coli O157:H7	Outer membrane proteins	10^1 to 10^5 CFU/mL	2.9×10^2 CFU/mL	Impedimetric aptasensor	(Brosel-Oliu et al., 2018)
2.	ATCCGTCACACCTGCTCTGTCTGCGAGCGGGGCGCGGGCCCGGC GGGGGATGCGTGGTGTTGGCTCCCGTAT	DNA	E. coli O157:H7	–	500 to 5x10^7 CFU/mL	250 and 400 CFU/mL, for buffer and milk samples respectively	Eye-based microfluidic aptasensor (EA-Sensor)	(Li et al., 2020)
3.	CCATGAGTGTTGTGAAATGTTGGGACACTAGGTGGCATAGAGC CG-C$_6$-SH	DNA	E. coli	–	3.2×10^1 to 3.2×10^7 CFU/mL	3.46 CFU/mL	SERS aptasensor	(Ye et al., 2022)
4.	Apt1 (signal probe) A20-CCGGACGCTTATGCCTTGCCATCTACAGAGCAGGTGTGACGG Apt2 (capture probe) biotin-CCGGACGCTTATGCCTTGCCATCTACAGAGCAGGTGTGACGG-3	DNA	E. coli O157:H7	–	10 to 10000 CFU/mL	3 CFU/mL	Gold nanobones enhanced ultrasensitive SERS aptasensor	(Zhou et al., 2020)
5.	CAG TCC AGG ACA GAT TCG CGA G-N$_{45}$-CAC GTG GAT TTC ATT CAG CGA TT	ssDNA	E. coli O157:H7	–	–	1.46×10^3 CFU/mL	Aptamer-antibody sandwich assay	(Yu et al., 2018)
6.	ATCCAGAGTGACGCAGCA-(N45)- TGGACACGGTGGCTTAGT	DNA	E. coli O78: K80:H11	–	10^1 to 10^6 CFU/mL	10 CFU/mL	Bridged rebar graphene functionalized impedimetric aptasensor	(Kaur et al., 2017)
7.	ATCCAGAGTGACGCAGCA-(N45)-TGGACACG GTGGCTTAGT	ssDNA	E. coli O157:H7	–	10^0 to 10^5 CFU/mL	10 CFU/mL	Electrochemical aptasensor using boron-carbon nanorods decorated by nickel nanoparticles	(Kaur et al., 2020)
8.	P-CCG GAC GCT TAT GCC TTG CCA TCT ACA GAG CAG GTG TGA CGG	DNA	E. coli O157:H7	LPS of E. coli O157:H7	–	3 CFU/mL	Zirconium-based metal–organic frameworkTi$_3$C$_2$T$_x$ nanosheet based faraday cage-type electrochemical aptasensor	(Dai et al., 2022)
9.	SH-ATC CGT CAC ACC TGC TCT GTC TGC GAG CGG GGC GCG GGC CCG GCG GGG GAT GCG TGG TGT TGG CTC CCG TAT	DNA	E. coli O157:H7	–	500 to 5000 CFU/mL	116 CFU/mL	MoS$_2$ nanosheets-based label-free colorimetric aptasensor	(Li et al., 2023)
10.	TATGGCGGCGTCACCCGACGGGGACTTGACA TTATGACAG	DNA	Salmonella enterica	–	10^8 to 10^1 CFU/mL	10^1 CFU/mL	Reduced graphene oxide-titanium dioxide nanocomposite-based electrochemical aptasensor	(Muniandy et al., 2019)
11.	–	dsDNA	Salmonella typhimurium	–	10 to 10^5 CFU/mL	6 CFU/mL	Aptasensor based immuno-HCR-SERS method with dual signal amplification capability	(Li et al., 2021)

(Continued)

TABLE 1 Continued

S.No.	Aptamer sequence (5′ to 3′)	Type	Organism	Target	Concentration range	LOD (limit of detection)	Methodology	Reference
Bacteria								
12.	C_6-NH_2-CTGTCATAAT GTCAAGTC	CdTe QD-labeled ssDNA2	*Salmonella typhimurium*	Outer membrane proteins	10 to 10^{10} CFU/mL	1 CFU/mL	Aptamer-based fluorescence assay	(Ren et al., 2019)
13.	ATTAGTCAAGAGGTAGACGCACATAAGGGGTCTGGTGTCGGGCCGC GGGTCAGGGGGGTAAGGGATTCTGGTCGTCGTGACTCCTAT	ssDNA	*Salmonella paratyphi A*	–	–	10 CFU/mL	FRET based aptasensor	(RM et al., 2020)
14.	Apt1 botin- GAGGAAAGTCTATAGCAGAGGAGATGTGTGAACCGAGTAA Apt2 CTCCTCTGACTGTAACCACGGAGTTAATCAATACAAGGCGGGAACA TCCTTGGCGGTGCCGCATAGGTAGTCCAGAAGCC	ssDNA	*Salmonella typhimurium*	–	3.3×10^1 to 3.3×10^6 CFU/mL	33 CFU/mL in pure culture and 95 CFU/mL in spiked milk	Colorimetric sensor based on dual aptamers - the absorbance intensity ratio (A_{523}/A_{650}) for quantitative analysis of various concentrations of bacteria	(Chen et al., 2021a)
15.	TAT GGC GGC GTC ACC CGA CGG GGA CTT GAC ATT ATG ACA G	DNA	*Salmonella typhimurium*	–	10 to 10^5 CFU/mL	4 CFU/mL	SERS using spiny gold nanoparticles (SGNPs)	(Ma et al., 2018)
16.	Apt 1 SH-AGTAATGCCCGGTAGTTATTCAAAGATGAGTAGGAAAAGA Apt2 ROX-AGTAATGCCCGGTAGTTATTCAAAGATGAGTAGGAAAAGA	DNA	*Salmonella typhimurium*		15 to 1.5×10^6 CFU/mL	15 CFU/mL	SERS-*S.typhimurium* specifically interacted with the aptamers to form Au@Ag-apt 1-target-apt 2-ROX sandwich-like complexes.	(Duan et al., 2016)
17.	HS-TATGGCGGCGTCACCCGACGGGGACTTGACATTATGACAG	ssDNA	*Salmonella enterica*		10 to 10^5 CFU/mL	1.223 CFU/mL	Competitive voltammetric aptasensor based on electrospun carbon nanofibers-gold nanoparticles modified graphite electrode	(Fathi et al., 2020)
18.	NH_2-TTT GGT CCT TGT CTT ATG TCC AGA ATG CGA GGA AAG TCT ATA GCA GAG GAG ATG TGT GAA CCG AGT AAA TTT CTC CTA CTG GGA TAG GTG GAT TAT	DNA	*Salmonella typhimurium*		10^1 to 10^8 CFU/mL	6 CFU/mL	Diazonium-based impedimetric aptasensor	(Bagheryan et al., 2016)
19.	NH_2-TAT GGC GGC GTC ACC CGA CGG GGA CTT GAC ATT ATG ACA-G	DNA	*Salmonella*		75 to 7.5×10^5 CFU/mL	25 CFU/mL	Impedimetric aptasensor using a glassy carbon electrode modified with an electrodeposited composite consisting of reduced graphene oxide and carbon nanotubes	(Jia et al., 2016)
20.	SH-GCA ATG GTA CGG TAC TTC CTC GGC ACG TTC TCA GTA GCG CTC GCT GGT CAT CCC ACA GCT ACG TCA AAA GTG CAC GCT ACT TTG CTA A	DNA	*S. aureus*		10^1–10^7 CFU/mL	1 CFU/mL	Dual recognition aptasensor	(El-Wekil et al., 2022)

(Continued)

TABLE 1 Continued

S.No.	Aptamer sequence (5′ to 3′)	Type	Organism	Target	Concentration range	LOD (limit of detection)	Methodology	Reference
				Bacteria				
21.	SH-TCG GCA CGT TCT CAG TAG CGC TCG CTG GTC ATC CCA CAG CTA CGT C	DNA	S. aureus		1.2×10^1 to 1.2×10^8 CFU/mL	1 CFU/mL	Electrochemical aptasensor using Au nanoparticles/carbon, nanoparticles/cellulose, nanofibers nanocomposite	(Ranjbar and Shahrokhian, 2018)
22.	GCG CCC TCT CAC GTG GCA CTC AGA GTG CCG GAA GTT CTG CGT TAT	DNA	S. aureus		10^8 to 10^1 CFU/mL	10 CFU/mL	Aptasensor based on the FRET between green carbon quantum dot and gold nanoparticle	(Pebdeni et al., 2020)
23.	ATACCAGCTTATTCAATTAGCAACATGAGGGGGATAGAGGGGGT GGGTTCTCTCGGCT	DNA	S. aureus	Targets protein A (surface bound virulence factor	–	10 CFU/mL	Impedimetric biosensor based on the protein A-binding aptamer	(Reich et al., 2017)
24.	–	DNA	MRSA	–	10^2 to 10^8 CFU/mL	Theoretical value = 2 CFU/mL Visual LOD <100 CFU/mL	Aptasensor swab designed for qualitative and quantitative detection, on contaminated non-absorbable surfaces.	(Raji et al., 2021)
25.	GCAATGGTACGGTACTTCCTC GGCACGTTCTCAGTAGCGCTCGCTGG TCATCCCACA GCTACGTCAAAAGTGCACGCTACTTTGCTAA	DNA	S. aureus	–	52 to 5.2×10^7 CFU/mL	1 CFU/mL	An ultrasensitive sandwich–type electrochemical aptasensor using silver nanoparticle/titanium carbide nanocomposites	(Hui et al., 2022)
26.	–	–	S. aureus	–	7.6×10^1 to 7.6×10^7 CFU/mL	1.09 CFU/mL	Dual-recognition SERS biosensor based on teicoplanin functionalized gold-coated magnet NPs as capture probe and S.aureus aptamer functionalized silver coated gold NPs as signal probe	(Qi et al., 2022)
27.	NH$_2$- GCG CCC TCT CAC GTG GCA CTC AGA GTG CCG GAA GTT CTG CGT TAT	DNA	S. aureus	–	10^2 to 10^8 CFU/mL	80 CFU/mL	Aptamer and antibiotic-based dual detection sensor combining vancomycin-copper nanoclusters for the recognition and quantification using fluorescence	(Bagheri Pebdeni et al., 2021)
28	–	DNA	S. aureus	–	10 to 10^8 CFU/mL	3 CFU/mL	Electrochemical aptasensor based on gold/nitrogen-doped carbon nano-onions	(Sohouli et al., 2022)

(Continued)

TABLE 1   Continued

S.No.	Aptamer sequence (5′ to 3′)	Type	Organism	Target	Concentration range	LOD (limit of detection)	Methodology	Reference
				Bacteria				
29.	ATCCATGGGGCGGAGATGAGGGGGAGGAGGGCGGGTACCCGGTTGAT	ssDNA	*Listeria monocytogenes*	–	1.4×10^1 to 1.4×10^6 CFU/mL	4 CFU/mL	Solid-state electrochemiluminescence biosensing based on the quenching effect of ferrocene on ruthenium pyridine	(Chen et al., 2021c)
30.	NH2-ATC CAT GGG GCG GAGATG AGG GGG AGG AGG GCG GGT ACC CGG TTGAT	ssDNA	*Listeria monocytogenes*	–	10^1 to 10^8 CFU/mL	10 CFU/mL	Paper-based electrodes conjugated with tungsten disulfide nanostructure and aptamer for impedimetric detection	(Mishra et al., 2022)
31.	biotin-ATC CAT GGG GCG GAG ATG AGG GGG AGG AGG GCG GGT ACC CGG TTG AT	DNA	*Listeria monocytogenes*	–	1.0×10^1 to 1.0×10^5 CFU/mL	6 CFU/mL	Luminol-functionalized AuNF-labeled aptamer recognition and magnetic separation	(Chen et al., 2021b)
32.	–	–	*Listeria monocytogenes*	–	10^2 to 2×10^8 CFU/mL	2.8×10^2 CFU/mL	Sandwich fluorometric method for dual-role recognition was developed based on antibiotic-affinity strategy and fluorescence quenching effect	(Li et al., 2022)
33.	biotin-TAC TAT CGC GGA GAC AGC GCG GGA GGC ACC GGG GA	DNA	*Listeria innocua*	–	–	1.6×10^3 CFU/mL	Acoustic aptasensor	(Oravczová et al., 2020)
34.	TATCCATGGGGCGGAGATGAGGGGGAGGAGGGCGGGTACCCGGTTGAT	DNA	*Listeria monocytogenes*	–	4.6×10^2 to 4.6×10^7 CFUmL^{-1} in pure culture and 6.1×10^3 to 6.1×10^7 CFU/g in spiked fresh lettuce	4.6×10^2 CFUmL^{-1} in pure culture and 6.1×10^3 CFU/g in spiked fresh lettuce	Competitive enzyme-linked aptasensor with rolling circle amplification (ELARCA) assay for colorimetric detection	(Zhan et al., 2020)
35.	TACTATCGCGGAGACAGCGCGGGAGGCACCGGGGA	–	*Listeria monocytogenes*	–	1.4×10^1 to 1.4×10^7 CFUmL	0.88 CFU/mL	Dual recognition and highly sensitive detection by fluorescence enhancement strategy	(Du et al., 2022)
36.	NH2(CH2)6GGGAGCTCAGAATAAACGCTCAA TACTATCGCGGGACAGCGC GGGAGGCACCGGGGATTCGACATGAGGCCCGGATC	DNA	*Listeria monocytogenes*	–	68 to 68×10^6 CFU/mL	8 CFU/mL	Fluorescence aptasensor	(Liu et al., 2021)
37.	NH2-C6-CCC CCG TTG CTT TCG CTT TTC CTT TCG CTT TTG TTC GTT TCG TCC CTG CTT CCT TTC TTG	DNA	*Pseudomonas aeruginosa*	–	3.1×10^2 to 3.1×10^7 CFU/mL	100 CFU/mL	Low-field magnetic resonance imaging aptasensor for the rapid and visual sensing	(Jia et al., 2021)
38.	NH2- CCC CCG TTG CTT TCG CTT TTC CTT TCG CTT TTG TTC GTT TCG TCC CTG CTT CCT TTC TTG	DNA	*P. aeruginosa*	Whole cell	10^2 to 10^6 CFU/mL	50 CFU/mL	A magnetic relaxation switch aptasensor	(Jia et al., 2017)

(Continued)

TABLE 1 Continued

S.No.	Aptamer sequence (5′ to 3′)	Type	Organism	Target	Concentration range	LOD (limit of detection)	Methodology	Reference
				Bacteria				
39.	CCCCCG TTGCTTTCGCTTTTCCTTTCGCT TTTGTTCGTTTC GTCCCTGCTTCCTTTCTTG	ssDNA	*P. aeruginosa*	–	10^8 to 10^5 CFU/mL	10^5 CFU/mLfor colour change by the naked eye and 10^4 CFU/mL for UV–Vis spectrometry	Colorimetric detection by aptamer–functionalized gold nanoparticles	(Schmitz et al., 2023)
40.	GCA-ATG-GTA-CGG-TAC-TTC-CCG-GGG-CCC-GCT-TCT-GGT-GCG-GTG -TAC-TAG-TGA-CCG-CAA-AAG-TGC-ACG-CTA-CTT-TGC-TAA-(CH$_2$) 6-SH	DNA	*P. aeruginosa*	3-O-C12-HSL (Quorum-Sensing Molecule)	0.5 to 30 µM	0.5 µM	Label-free electrochemical aptasensor for the detection of the 3-O-C12-HSL	(Capatina et al., 2022)
41.	CCC CCG TTG CTT TCG CTT TTC CTT TCG CTT TTG TTC GTT TCG TCC CTG CTT CCT TTC TTG	DNA	*P. aeruginosa*	–	1.28×10^3 to 2.00×10^7 CFU/mL	100 CFU/mL	Graphene oxide quantum dots assisted construction of fluorescent aptasensor	(Gao et al., 2018)
42.	NH2-CCC CCG TTG CTT TCG CTT TTC CTT TCG CTT TTG TTC GTT TCG TCC CTG CTT CCT TTC TTG	DNA	*P. aeruginosa*	–	10^2 to 10^7 CFU/mL	33 CFU/mL	Impedimetric aptasensor by using a glassy carbon electrode modified with silver nanoparticles	(Roushani et al., 2019)
				Virus				
43.	AGC GGA TCC GAT GGG TGG GGG GGT GGG TAG GAT CCG CG	ssDNA	DENV	Non-structural protein 1	–	2.51 nM in buffer and 8.13 nM in serum	G-quadruplex (GQ)-based fluorescent aptasensor using one-shot detection of NS1	(Mok et al., 2021)
44.	HS_TAGGCAGTGTGGACGAGAGGGAGCTGTCCTGAGAGAGGCCTG TCAACCAGGGGTACCACAACCGAGGGCATA_SH	DNA	DENV-2	E-protein	–	100 infectious units per mL	Porous Au-seeded Ag nanorod networks conjugated with DNA aptamers for impedimetric sensing	(Kumar De et al., 2021)
45.	–	DNA	DENV	surface envelope proteins	10^{-6} to 10^6 TCID$_{50}$ /mL	1.74×10^{-7} TCID$_{50}$/mL	AC-electrothermal flow-based rapid biosensor	(Park et al., 2023)
46.	HS(CH$_2$)$_6$ – TTTTT – ACTAGGTTGCAGGGGACTGCTCGGGATTGCG GATCAACCTAGTTGCTTCTCTCGTATGAT	DNA	DENV-1 and DENV-4	NS1	10 pg to 1 µg/mL	22 pg/mL	Electrochemical aptasensor	(Bachour Junior et al., 2021)
47.	–	DNA	Hepatitis C virus (HCV)	HCV core protein	10 to 70 pg/mL and 70 to 400 pg/mL	3.3 pg/mL	Electrochemical detetction using GQD nanocomposite	(Bachour Junior et al., 2021)

(Continued)

TABLE 1 Continued

S.No.	Aptamer sequence (5' to 3')	Type	Organism	Target	Concentration range	LOD (limit of detection)	Methodology	Reference
Virus								
48.	GCGGATCCAGACTGGTGTGCCGTATCCCT CCCTTGTAATTATTTG TTCCATCCGTTCCGCCCTAAAGACAAGCTTC	ssDNA	HCV	HCV core protein	10^{-14} to 10^{-18} M	15.6 aM	Attomolar detection powered by molecular antenna-like effect in a graphene field-effect aptasensor	(Palacio et al., 2023)
49.	CACAGCGAACAGCGGCGGACATAATAGTGCTTACTACGAC	DNA	Hepatitis B virus (HBV)	HBsAg	–	0.05ng/mL	Chemiluminescent aptasensor based on rapid magnetic separation and double-functionalized gold nanoparticle	(Xi et al., 2018)
50.	NH_2- TTGGGGTTATTTGGGAGGGCGGGGGTT	DNA	Influenza A virus	H5N1 IAV hemagglutinin	0.2 to 12 ng/mL	114.7 pg/mL	FRET Aptasensors	(Zhao et al., 2021)
51.	GTG TGC ATG GAT AGC ACG TAA CGG TGT AGT AGA TAC GTG CGG GTA GGA AGA AAG GGA AAT AGT TGT CCT GTT G	DNA	H5N1 AIV	–	–	0.0128 hemagglutinin units (HAU)	An Impedance Aptasensor with Microfluidic Chips	(Lum et al., 2015)
52.	Cy3/GGG TTT GGG TTG GGT TGG GTT TTT GGG TTT GGG TTG GGT TGG GAA AAA	DNA	Influenza A/ H1N1 virus	–	–	97 PFU/mL	SERS imaging-based aptasensor	(Chen et al., 2020)
53.	Apt 1 H2N-GCT AGC GAA TTC CGT ACG AAG GGC GAA TTC CAC ATT GGG CTG CAG CCC GGG GGA TCC Apt 2 H2N-GTC TGT AGT AGG GAG GAT GGT CCG GGG CCC CGA GAC GAC GTT ATC AGG C Apt 3 H2N-CGT ACG GAA TTC GCT AGC ACG GGG CTT AAG GAA TAC AGA TGT ACT ACC GAG CTC ATG AGG ATC CGA GCT CCA CGT G Apt 4 H2N-CGT ACG GAA TTC GCT AGC CGA CGG TCA ATG CTC GTG AGC CAG TAC ACA CAA TAT ATG TGG ATC CGA GCT CCA CGT G	DNA	Norovirus	NoV capsid protein	–	70 aM	An Aptamer-aptamer Sandwich Assay with Nanorod-enhanced SPR for Attomolar Concentration	(Kim et al., 2018b)
54.	AGT ATA CGT ATT ACC TGC AGC CCA TGT TTT GTA GGT GTA ATA GGT CAT GTT AGG GTT TCT GCG ATA TCT CGG AGA TCT TGC	DNA	Norovirus	–	13 ng/mL to 13 µg/mL	4.4 ng/mL and 3.3 ngmL for MWCNT or GO respectively	Aptamer-based fluorometric determination using a paper-based microfluidic device	(Weng and Neethirajan, 2017)
55.	GCTAGCGAATTCCGTACGAAGGGCGAATTCCACATTGGGCT GCAGCCCGGGG GATCC	DNA	Norovirus	MNV virion	–	200 viruses/mL	Ultrasensitive colorimetric detection using NanoZyme aptasensor	(Weerathunge et al., 2019)

(Continued)

TABLE 1 Continued

S.No.	Aptamer sequence (5′ to 3′)	Type	Organism	Target	Concentration range	LOD (limit of detection)	Methodology	Reference
			Virus					
56.	CAG CAC CGA CCT TGT GCT TTG GGA GTG CTG GTC CAA GGG CGT TAA TGG ACA	DNA	SARS-CoV-2-RBD	–	0.5–250 ng/mL	32 ng/mL	Highly sensitive aptasensor using aptamer-gated methylene blue@mesoporous silica film/laser engraved graphene electrode	(Amouzadeh Tabrizi and Acedo, 2022)
57.	–	DNA	SARS-CoV-2	Nucleocapsid protein	–	0.77 to 1.94 ngmL	Fluorescent nanodiamond-based spin-enhanced lateral flow immunoassay and spike protein from different variants	(Wei-Wen Hsiao et al., 2022)
58.	Apt 1 biotin-GCT GGA TGT CAC CGG ATT GTC GGA CAT CGG ATT GTC TGA GTC ATA TGA CAC ATC CAG C Apt 2 biotin-GCT GGA TGT TGA CCT TTA CAG ATC GGA TTC TGT GGG GCG TTA AAC TGA CAC ATC CAG C	DNA	SARS-CoV2	Nucleocapsid protein	–	33.28 pg/mL	Aptamer/antibody sandwich method	(Ge et al., 2022)
59.	GCA ATG GTA CGG TAC TTC CGG ATG CGG AAA CTG GCT AAT TGG TGA GGC TGG GGC GGT	DNA	SARS-CoV-2	–	1 fM to 100 pM	0.389 fM	Aptasensing nucleocapsid protein on nanodiamond assembled gold interdigitated electrodes for impedimetric assessment	(Ramanathan et al., 2022)
60.	TGA CAC CGT ACC TGC TCT-N40-AAG CAC GCC AGG GAC TAT	DNA	Zika virus	–	100 pM to 10 μM	38.14 pM	Electrical biosensor	(Park et al., 2022)
61.	CTTCTGCCCGCCTCCTTCC-(39N)-GGAGACGAGATAGGCGGACACT	DNA	Zika virus	NS1 protein	0.01 to 1000 pg/mL	0.01 pg/mL	Aptasensor based on graphene FETs	(Almeida et al., 2022)

3.2 Electrochemical biosensors

A variety of electrochemical transducer systems, including impedimetric, potentiometric, amperometric, voltammetric, conductometric, and FET-based biosensors, can be integrated with aptamers for enhanced functionality.

3.2.1 Impedimetric aptasensor

When the target analyte binds to the aptamer functionalized sensor surface, inducing changes in the electrical properties at the interface such as charge transfer kinetics, dielectric properties, or surface conductivity at the sensor interface. The change in impedance is converted into a measurable electrical signal. Impedance spectroscopy measures the impedance change of the sensor due to exposure to the target analyte and computes how the sensors electrical impedance changes over a range of frequencies. In a study conducted by Roushani et al. (2019) NH_2-aptamer was immobilized covalently on the surface of a glassy carbon electrode through electrodeposition modification of AgNPs. The conductivity and the charge transfer resistance before and after the addition of $P.aeruginosa$ to the aptasensor was studied. The impedance increases on going from 10^2 to 10^7 CFU/mL concentrations of $P.\ aeruginosa$, and the detection limit was found to be 33 CFU/mL (for S/N=3). In a study conducted by Ramanathan et al. (2022) carbon nanodiamond enhanced gold interdigitated electrode was used to detect the nucleocapsid protein of SARS-CoV-2. The aptasensor which was portable, showed a good selectivity with a lower detection limit of 0.389 fM; at a linear detection range from 1 fM to 100 pM; showing 30 & 33% loss with stability & reusability. A rapid (30 mins) label-free aptasensor was constructed by Bagheryan et al., using screen-printed electrodes (SPEs) that were modified with diazonium salt for the detection of $Salmonella\ typhimurium$ in spiked apple juice samples. The aptasensor had a linear detection range of 1×10^1 to 1×10^8 CFU mL^{-1} (Bagheryan et al., 2016).

3.2.2 Voltammetry based aptasensors

In a recent study, Fathi et al. (2020) developed a novel voltammetric aptasensor for detecting $Salmonella\ enterica$ serovar. The sensor utilized a pencil graphite electrode modified with chitosan-coated electrospun carbon nanofibers and gold nanoparticles. The presence of the analyte on the electrode surface led to an increase in charge transfer resistance, with the change in current being measured as a function of voltage. Electrochemical detection of $Salmonella$ was achieved using differential pulse voltammetry in a methylene blue solution. The aptasensor demonstrated a linear detection range of 10 to 10^5 CFU/mL, with a limit of detection (LOD) of 1.223 CFU/mL, outperforming the PCR technique.

3.2.3 Graphene FET based aptasensors

An aptamer with high affinity against HCV (hepatitis C virus) was functionalized on graphene solution-gated field-effect transistors (g-SGFET) and the developed aptasensor was used to amplify and detect the change in conductance caused by the interaction between the aptamer and the HCV core protein (Palacio et al., 2023). Similarly, Almeida et al., fabricated a graphene FET aptasensor to detect Zika virus (ZIKV). The aptamer (termed ZIK60), selected by CE-SELEX was complimentary to the Zika virus non-structural protein 1 (NS1) and counterselection against the NS1 proteins of DENV (serotypes 1, 2, 3, and 4) and YFV (Almeida et al., 2022).

3.2.4 Quartz crystal microbalance based aptasensors

QCM aptasensor is an acoustic (mass-based) piezoelectric biosensor that detect changes in mass on the aptamer immobilized surface of quartz crystal due to its interaction with the analyte molecules by detecting changes in the resonance frequency of the crystal. QCM-based aptasensors are highly sensitive, label free, portable and can be miniaturised and hence are suitable for point-of-care diagnostics. Aptamer selected using whole cell SELEX was utilized to fabricate a QCM sensor to detect $E.\ coli\ O157:H7$. The aptasensor had a LOD that was as low as 1.46×10^3 CFU/mL and outperformed most QCM-based immunosensors for pathogen detection. In addition, the quick response time of 50 min showed the possibility of using this aptamer in various other types of biosensors used for rapid detection and investigation of $E.\ coli$ O157:H7 outbreaks (Yu et al., 2018). An interesting study conducted by Wang et al., demonstrates the use of QCM based SELEX to effectively select the ssDNA aptamer and subsequent construction of QCM based aptasensor which was able to detect 10^3 CFU/mL of $S.\ typhimurium$ within 1 h (Wang et al., 2017a). Another example is a QCM aptasensor in which a nanowell based electrode effectively increased the immobilization capacity of aptamers for the detection of avian influenza virus. The result showed that the binding of target AIV H5N1 onto the immobilized aptamers decreased the sensor's resonant frequency, and the frequency change correlated to the virus titer. The detection range of 2^{-4} to 2^4 hemagglutination units (HAUs)/50 μL was obtained with a detection limit of 2^{-4} HAU/50 μL for AIV H5N1 with a detection time of 10 mins using a label free assay. (Wang et al., 2017a, 2017b)

3.3 Dual recognition aptasensor

As the name suggests, dual recognition sensors make use of two different recognition principles facilitating a highly specific detection. Li et al., developed an aptasensor for detecting $S.\ typhimurium$ by combining the methods of immune hybridization chain reaction (HCR) with SERS achieving double amplification and high sensitivity with a limit of detection of 6 CFU/mL in 3.5 h (Li et al., 2021). Bagheri Pebdeni et al., proposed an aptamer and antibiotic-based dual detection sensor that combines copper nanoclusters (CuNCs) as an effective approach for the recognition and quantification of $S.\ aureus$. The use of dual receptors enhanced fluorescence signal linearly with $S.\ aureus$ concentrations between 10^2 -10^8 CFU/mL, and the detection limit was 80 CFU/mL after 45 min (Bagheri Pebdeni et al., 2021).

Aptasensors like the electrochemiluminescence aptasensors come under both electrochemical and optical sensors. It works by detecting the luminescence that is produced due to the electrochemical interactions between the aptamer and the analyte molecules (Chen et al., 2021c; Chen et al., 2021b).

3.4 Sandwich assay based aptasensors

A sandwich assay involves two aptamers – the capture probe and the signal probe. The capture probe is immobilized on the surface of the sensor and after the analyte is added, the signal probe is added forming an aptamer-aptamer sandwich platform. This method is desirable because of the high sensitivity and selectivity that it offers. S. Kim et al., demonstrated a nanorod enhanced SPR with sandwich enzyme-linked immunosorbent assay (ELISA) for the attomolar detection of the norovirus (NoV) capsid protein (Kim et al., 2018b). RNA aptamer-based sandwich assays were used to detect the NS1 protein of dengue virus serotype 2 and a LOD of 2 nM was attained (Thevendran et al., 2023).

Another notable example is an aptamer/antibody sandwich constructed by Ge et al., for the digital detection of SARS-CoV2 nucleocapsid protein using fluorometry. The detection limit of this digital method for N protein was 33.28 pg/mL, which was 300 times lower than traditional double-antibody sandwich-based ELISA (Ge et al., 2022). Even though sandwich ELISA assay offers various advantages, it has a complex workflow, more optimization is required, is labor intensive and the time of detection is a little high.

3.5 Other aptasensors

There are aptasensors based on principles other than the above mentioned, for example, F. Jia et al. developed a low-field magnetic resonance imaging (LF-MRI) aptasensor based on the difference in magnetic behavior of two magnetic nanoparticles covalently immobilized with aptamers for the rapid detection of *P.aeruginosa*. Under optimum conditions, the LF-MRI platform provides both image analysis and quantitative detection of *P. aeruginosa*, with a detection limit of 100 CFU/mL (Jia et al., 2021).

Aptamer-based assays represent a significant advancement in the diagnostics of infectious diseases, addressing the limitations of traditional methods. Optical aptasensors, including surface plasmon resonance, fluorescence, and surface-enhanced Raman scattering, excel in sensitivity and specificity, ideal for detailed biomolecule detection. Electrochemical aptasensors, such as impedimetric, voltammetric, and graphene FET-based sensors, offer robust, portable solutions with high sensitivity for point-of-care applications. Meanwhile, dual-recognition and sandwich assay-based aptasensors combine multiple detection principles to enhance accuracy and detection limits. This comprehensive range of aptamer-based technologies demonstrates their potential to revolutionize diagnostic practices by providing versatile, efficient, and precise tools for infectious disease management. The most suitable method can be selected by understanding the strengths and limitations for each approach.

4 Notable aptasensor case studies

4.1 For the detection of methicillin resistant *Staphylococcus aureus-contaminated* surfaces

Methicillin-resistant Staphylococcus aureus (MRSA) is a well-known pathogen that causes healthcare-associated infections. Hospitals with contaminated environments are important sources for the spread of MRSA and other nosocomial infections. In a study, researchers have developed a new swab called a pathogen aptasensor which can specifically detect MRSA on contaminated non-absorbable surfaces. The visual detection limit of the MRSA aptasensor swab was less than 100 CFU/mL, and theoretically, using a standard curve, it was 2 CFU/mL. The assay has a short turnaround time of 5 minutes, with a linear range of quantitation from 10^2 to 10^5 CFU/mL. The MRSA aptamers bind to the swab's activated aldehyde group, and when exposed to an MRSA-contaminated surface, the activated nanobeads conjugate with the aptamer, causing the swab to turn blue. The intensity of the color change is proportional to the concentration of MRSA, allowing for both qualitative and quantitative detection (Raji et al., 2021).

4.2 Simultaneous detection of *E.coli* O157:H7 and *S.typhimurium*

Simultaneous detection of *E.coli* and *S.typhimurium* was achieved using an evanescent wave dual-color fluorescence aptasensor based on time resolved effect. Two fluorescence labeled aptasensors, Cy3-apt-E and Cy5.5-apt-S that were complimentary to *E.coli* O157:H7 and *S.typhimurium* were alternatively excited by evanescent waves originated from 520 nm to 635 nm excitation lights, respectively. The fiber nanoprobe with *in-situ* etched nanopores was used for distinguishing free aptamer and aptamers bound to pathogenic bacteria based on the limited penetrated depth of evanescent wave and the significant size difference of bacteria and nanopore. The *E. coli* O157:H7 and *S. typhimurium* were directly and simultaneously quantitated in less than 35 min without the requirement of the complex immobilization of biorecognition molecules and bacteria enrichment/separation processes. The limits of detection of *E. coli* O157:H7 and *S. typhimurium* were 340 CFU/mL and 180 CFU/mL, respectively (Fang et al., 2021).

4.3 Colorimetric aptasensor for detecting *Salmonella* spp., *Listeria monocytogenes*, and *Escherichia coli* in meat samples

Aptasensors are revolutionizing infectious disease detection by enhancing the specificity and sensitivity of aptamers. These biosensors provide versatile solutions for streamlining diagnostic processes in healthcare by rapidly and precisely identifying pathogens.

A recent study introduced a quick detection method that can simultaneously identify *Salmonella* spp., *Listeria monocytogenes*,

and *E. coli*. This method uses visual colorimetric detection with labeled colloidal gold nanoparticles and UV absorbance determination at optimized wavelengths of 625 nm and 525 nm. The aptasensor has a detection limit as low as 10^5 CFU/mL. Notably, this colorimetric aptasensor enables one-step detection without the need for pre-culture, DNA extraction, or amplification steps. As a result, it provides a simple, rapid, specific, and qualitative assay suitable for point-of-care testing, allowing for direct detection of multiple foodborne pathogens (Ledlod et al., 2020). Additionally, exploring virulence factors as potential targets for aptamers is helping us understand pathogen behavior and leading to the development of targeted therapeutic interventions.

5 Aptamer applications: targeting virulence factors and recent advances

5.1 Virulence factors and potential aptamer targets

Aptamer is one of the most promising therapeutic candidates because of its selectivity. In the field of therapeutics, they serve various crucial roles, including acting as a drug delivery vehicle (Ninomiya et al., 2014), functioning as a targeting molecule for genes or whole cells, thereby reducing the expression of virulent genes in pathogens and enhancing susceptibility to the immune system (Lai et al., 2014). Furthermore, it serves as a binding agent for toxins and specific proteins that contribute to increased pathogen virulence (Gribanyov et al., 2021). When it comes to treating viral infections that have no known treatment and drug-resistant microorganisms that cause infectious diseases, aptamers may be a useful therapeutic tool (Figure 3).

5.1.1 Bacteria

By removing important virulence components from bacteria, aptamers present a viable strategy for treating bacterial illnesses. (Tables 2, 3). The innovative technology enhance the treatment efficacy against pathogens such as *Staphylococcus aureus*, *Mycobacterium tuberculosis*, *Salmonella typhi*, *Listeria monocytogenes*, *Streptococcus pneumoniae*, and *Escherichia coli*. In the fight against *S. aureus* infections, aptamers AT-33 and AT-36 have been specifically engineered to target and neutralize the α-toxin, a key virulence factor. These aptamers effectively inhibit α-toxin-induced cell death and cytokine upregulation in human cells, offering a promising therapeutic approach (Ommen et al., 2022). Another set of aptamers targets *S. aureus* biofilms, binding to the biofilm matrix to enhance antibiotic delivery and significantly improve treatment outcomes by overcoming biofilm-associated resistance. This dual approach of targeting both toxins and biofilms represent a significant advancement in therapeutic strategies against *S. aureus* infections.

To identify and target important molecules connected to M. tuberculosis, aptamers have also been developed. For instance, mannose-capped lipoarabinomannan (ManLAM), a major glycolipid on the bacterial surface, serves as a target for specific aptamers, aiding in both diagnostic and therapeutic applications.

Additionally, aptamers targeting the GlcB and HspX antigens disrupt bacterial metabolism and persistence, offering potential therapeutic benefits (Zhou et al., 2021). Furthermore, aptamers targeting ESAT-6, a critical virulence factor secreted by *M. tuberculosis*, can reduce the bacterium's virulence and increase its vulnerability to immune system attacks (Sreejit et al., 2014). *M. tuberculosis* produces a lipid called phthiocerol dimycocerosate (PDIM), which is essential to the pathogenicity and virulence of the bacteria (Augenstreich et al., 2020).

Researchers have developed an aptamer that interacts with and neutralizes the InvA gene of *S. typhi*, a crucial element in the bacterium's invasion process. Additionally, the S9 aptamer targets the outer membrane protein of *S. typhi*, further contributing to the bacterium's neutralization (Pathania et al., 2017; Yang et al., 2013). SPI1, or *Salmonella* pathogenicity island 1, is essential for *Salmonella's* interaction with host cells, facilitating penetration through the T3SS, also known as the needle complex, which assembles proteins to translocate effector proteins into host cells (Raffatellu et al., 2005; Lerminiaux et al., 2020). The pathogenicity of *S. typhi* is enhanced by the release of typhoid toxin and the Vi capsular antigen, which has anti-opsonic and antiphagocytic properties (Galán, 2016; Tran et al., 2010; Wain et al., 2005). These harmful factors can be targeted by specifically curated aptamers.

In order to prevent L. monocytogenes from invading host cells, aptamers that target InlB, one of the bacteria's virulence factors, have been created. By blocking this key infection pathway, these aptamers offer a promising therapeutic strategy for preventing *L. monocytogenes* infections (Chen et al., 2024). *L. monocytogenes* produces listeriolysin O (LLO), a pore-forming toxin dependent on cholesterol (Dramsi and Cossart, 2002). LLO damages the vacuolar membrane, facilitating bacterial escape into the cytosol (Petrišič et al., 2021). These vulnerable parts of the pathogen can be exploited by targeting them with protein-specific aptamers.

For *S. pneumoniae*, aptamers have shown good specificity; the Lyd-3 aptamer in particular has shown promise. Lyd-3 effectively inhibits biofilm formation, a critical factor in the pathogen's virulence and antibiotic resistance. By significantly reducing biofilm formation, Lyd-3 enhances treatment outcomes, especially when used in combination with antibiotics (Afrasiabi et al., 2020). The pneumococcus's polysaccharide capsule is a significant virulence component, aiding in immune evasion and colonization (Jonsson et al., 1985). PspK mediates adherence to human epithelial cells, independent of the pneumococcal isolate genetic background (Keller et al., 2013).

Four aptamers have demonstrated high affinity and specificity for *E. coli* cells, making them valuable tools for both diagnostic and therapeutic applications. These aptamers offer precise detection and effective targeting of *E. coli* (Marton et al., 2016). *E. coli* causes various infections, including urinary tract infections, and relies on colonization factors and toxins for virulence. Aptamers can target these virulent factors, disrupting *E. coli*'s pathogenic mechanisms and enhancing treatment efficacy (Johnson, 1991; Kaper et al., 2004; Terlizzi et al., 2017).

By leveraging the specificity and affinity of aptamers, we can target key virulence factors in various bacterial pathogens, offering innovative and effective therapeutic strategies.
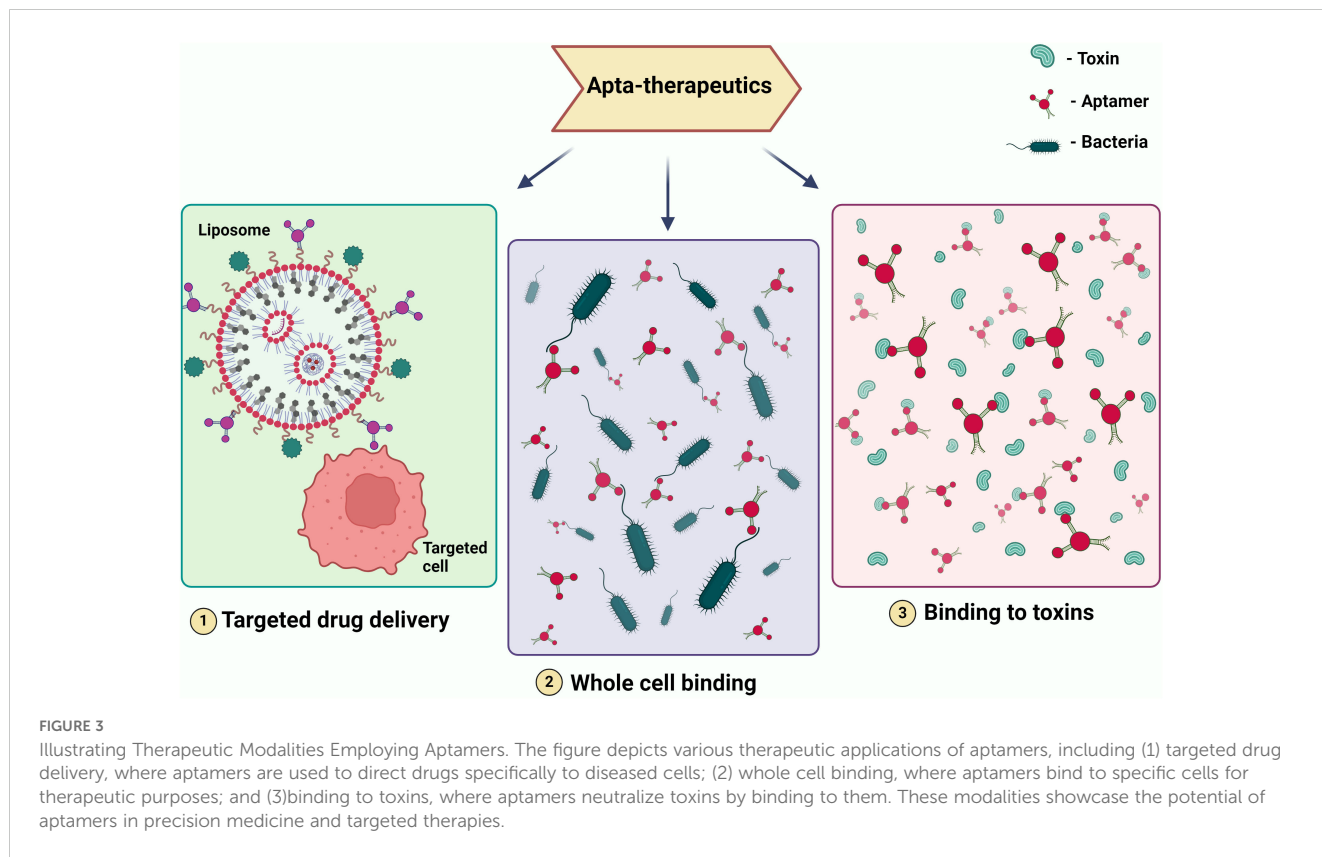
FIGURE 3
Illustrating Therapeutic Modalities Employing Aptamers. The figure depicts various therapeutic applications of aptamers, including (1) targeted drug delivery, where aptamers are used to direct drugs specifically to diseased cells; (2) whole cell binding, where aptamers bind to specific cells for therapeutic purposes; and (3)binding to toxins, where aptamers neutralize toxins by binding to them. These modalities showcase the potential of aptamers in precision medicine and targeted therapies.

TABLE 2 Therapeutic techniques and mechanisms of aptamers against bacteria.

Target	Conjugated With	Target site	Mechanism	Reference
Salmonella species				
S. choleraesuis	Ampicillin	Flagella	■ Aptamer 3 targets flagella, causing loss of bacterial motility decreasing adherence to the matrix surface, and reinforces hydrodynamic and repulsive forces which inhibit biofilm formation. ■ Aptamer 3 may also serve as an antibiotic carrier helping ampicillin to penetrate biofilms to eradicate bacteria and to overcome biofilm tolerance to drugs	(Lijuan et al., 2017)
S. enteritidis	–	Sip A protein (SPI – *Salmonella* pathogenicity island)	■ Apt17, an aptamer targeting SipA an effector protein secreted by Type Three Secretion System (T3SS). ■ It facilitates the invasion of *Salmonella* cells by triggering membrane ruffling	(Shatila et al., 2020b)
S. Typhimurium and S. Enteritidis	–	Sip A protein (SPI – *Salmonella* pathogenicity island)	■ Targeting *Salmonella* invasion protein (SipA) ■ A type three secretory system effector protein blocking this helps in anti-adhesion and anti-invasion property against *Salmonella Enteritidis*	(Shatila et al., 2020a)
S. Typhimurium and S. Enteritidis	Using rolling circle amplification	-	■ Use complementary sequences of recently described (anti-ST and anti-SE) DNA aptamers as a template to develop RCA-p. ■ The use of RCP-p is done to increase the bacteriostatic effect on the bacteria	(Hameed et al., 2022)
Salmonella enterica serovar typhimurium	Gold nano particles	Membrane disruption, Intracellular interaction.	■ Involve the binding of the AMPs to lipopolysaccharide and lipoteichoic acid ■ With subsequent membrane disruption through pore formation or other processes ■ AMPs are drugs delivered by aptamer nanoparticle complex	(Yeom et al., 2016)
Salmonella enterica Serovar typhi	–	Preferentially bind type IVB pilli	■ RNA Aptamer is used to bind to IVB pilus operon and stops IVB PILUS formation	(Pan et al., 2005)

(Continued)

TABLE 2 Continued

Target	Conjugated With	Target site	Mechanism	Reference
Salmonella species				
			▪ Which helps *S.enterica serovar typhi* to attach to cells which increases its pathogenicity	
Staphylococcus aureus				
S aureus	Teicoplanin and PLGA nanoparticles	D-Ala, D-Ala site in peptidoglycan	▪ Aptamer is used to bind to the bacteria and is conjugated with teicoplanin encapsulated in PLGA ▪ Which stops the cell wall synthesis by blocking the D-Ala, D-Ala site	(Ucak et al., 2020)
S. aureus	–	Alpha toxin and transcriptional activators of *TNF-alpha* and *IL 17* gene	▪ Aptamers are specific to their targets through SELEX process, so they bind directly to the alpha toxin	(Vivekananda et al., 2014)
S .aureus (MRSA)	Magnetic graphene oxide	Whole-cell	▪ The conjugated magnetic graphene oxide (MGO) benefits from the aptamer ▪ When it is exposed to NIR light, it produces heat that aids in the death of MRSA.	(A Ocsoy et al., 2021)
S aureus (MRSA)	Anti-galactosyltransferase (anti-α-gal)	Whole-cell and help immune system enhance the fight against *MRSA*	▪ Anti-galactosyltransferase, or anti-α-gal, is conjugated with MRSA specific aptamer. ▪ Anti-α-gal alerts the immune system to the presence of bacteria and aids in its prompt elimination.	(Doherty et al., 2023)
S aureus	NaY0.28F4:Yb0.70, Er0.02 magnetic nanoparticle	As of now no targets but This can be used as a potential therapeutic	▪ The magnetic nanoparticle NaY0.28F4:Yb0.70, Er0.02 coupled with aptamer is utilized to draw all of the bacterial cells into one location, offering it a possible therapeutic use.	(Duan et al., 2012)
Mycobacterium tuberculosis				
Mycobacterium tuberculosis	–	Malate Synthase	▪ Aptamer attaches itself to the Mtb's malate synthase, ▪ Inhibiting adhesin function and preventing bacterial invasion.	(Dhiman et al., 2019)
Mycobacterium tuberculosis	–	HupB protein	▪ Aptamer attaches itself to the HupB protein and prevents it from working.	(Kalra et al., 2018)
Mycobacterium tuberculosis	Biotin	DevR dimer	▪ The DevR dimer becomes dysfunctional when an aptamer attaches to it, inhibiting transcription.	(Chauhan et al., 2022)
Listeria monocytogenes				
Listeria monocytogenes	Porous silica Nanoparticles	Whole-cell	▪ The aptamer is coupled to porous silica nanoparticles and loaded with benzalkonium chloride (BAC). ▪ Because BAC is toxic, it cannot be utilized in treatment; instead, an appropriate antibiotic can be employed to effectively target the bacteria.	(Sudagidan et al., 2021)
Listeria monocytogenes	Antibody of *L. monocytogenes*	Antigen	▪ When an aptamer and bacterial antibodies are conjugated The antigen found in the bacterium may be targeted therapeutically.	(Du et al., 2022)
Listeria monocytogenes	Bacteriocin (nisin with leucocin F10)	Cell membrane	▪ Aptamer in connection with Nisin and Leucocin F10 Once it attaches to bacteria, the aptamer pores the bacteria's surface.	(Turgis et al)
Streptococcus pnuemoniae				
Streptococcus pnuemoniae	α-Gal epitope	Whole cell	▪ An aptamer is designed to attach to an α-Gal epitope, creating an alphamer that targets bacteria ▪ Initiating opsonization and phagocytosing the pathogen by anti-α-Gal antibody.	(Kristian et al., 2015)
Streptococcus pnuemoniae	Graphene oxide (GO)		▪ This aptamer has the potential to be a therapeutic tool when combined with drugs that are specific to this bacteria	(Bayraç and Donmez, 2018)
Streptococcus pnuemoniae	–	PavA and FHbp	▪ Researchers created an aptamer that binds to the virulent proteins PavA and FHbp. ▪ When the aptamer binds to PavA, it prevents the bacteria from attaching to fibronectin	(Escolano et al., 2017)

(Continued)

TABLE 2 Continued

Target	Conjugated With	Target site	Mechanism	Reference
Streptococcus pnuemoniae				
			▪ When it binds to FHbp, it compromises the ability to evade the immune system and kills the bacteria.	
Escherichia coli				
E. coli	–	Targets adhesins and colonization factor eg: Afimbrial Adhesins	▪ Aptamers were employed to lower the biofilm activity.	(Kusumawati et al., 2022)
E.coli	–	Cell membrane	▪ Aptamer was designed to attach to the elements of the cell membrane. ▪ It is also utilized to prevent from forming biofilms.	(Oroh et al., 2020)
E.coli	–	LPS	▪ This paper's researchers have inferred that aptamer attaches to the LPS ▪ This method may be exploited as a treatment option in addition to detection.	(Zou et al., 2018)
E.coli	AuNPs and Antimicrobial peptides	Cell membrane	▪ Antimicrobial action is demonstrated by HPA3P, a derivative of HP(2-20) ▪ AMP with substitutions of E9P connected with gold nanoparticles and aptamer pair (AuNPs-Apt).	(Lee et al., 2017)

TABLE 3 Virulence factors for aptamer-based targeting of bacterial pathogens.

Virulent factors	Bacteria						Reference
	L. monocytogenes	*S.aureus*	*S.typhi*	*M.tuberculosis*	*E.coli*	*S.pnuemoniae*	
LPS (Endotoxin)			+		+		(Chessa et al., 2014) (Somerville et al., 1999)
Colonization factor		+(adhesins)			+		(Gerlach et al., 2007) (Gerlach et al., 2007)
Listeriolysin O	+						(Portnoy et al)
Phospholipases	+	+					(Faucher et al., 2008) (Kadurugamuwa and Beveridge, 1995)
ACT A	+						(Pistor et al., 1994)
Capsules	+	+	+	+	+	+	(Bai et al., 2021)
Exotoxins	+(Listeriolysin O)	+ (hemolysin, leukotoxin, exfoliative toxin, enterotoxin, and toxic-shock syndrome toxin-1 (TSST-1).)	+(typhoid toxin)	+(necrotizing toxin)	+	+(pneuemolysin)	(Portnoy et al) (Otto, 2014) (Fowler and Galán, 2018) (Sun et al., 2015) (Kaper et al., 2004) (Nishimoto et al., 2020)
ESAT-6				+			(Sreejit et al., 2014)
Surface adhesins		+	+	+	+	+	(Gerlach et al., 2007) (Johnson, 1991)

(Continued)

TABLE 3 Continued

Virulent factors	Bacteria						
	L. monocytogenes	S.aureus	S.typhi	M.tuberculosis	E.coli	S.pnuemoniae	Reference
Protein A		+					(Palmqvist et al., 2002)
Salmonella pathogenicity island			+(SPI1, SPI2, SPI3)				(Lerminiaux et al., 2020)
Vi antigen			+				(Zhang et al., 2022)
Pneumococcal factors (*psp k , sir A, pmp A*)						+	(Brooks and Mias, 2018)
Flagella	+		+		+		(Winter et al., 2009) (Grü ndling et al., 2004)
Protein Kinases	+				+	+	(Wang & Koshland, 1978) (Canova and Molle, 2014)
Mannose capped lipoarabinomannan				+			(Turner and Torrelles)
Phthiocerol Dimycocerosate				+			(Augenstreich et al., 2020)

5.1.2 Virus

Aptamers are also increasingly recognized for their potential to combat viral infections by targeting and neutralizing specific viral components (Table 4). It can enhance the efficacy of existing antiviral treatments and provides new therapeutic avenues for diseases like Zika virus, Nipah virus, Ebola virus, and Influenza A virus.

Zika virus, a member of the Flaviviridae family transmitted by Aedes aegypti mosquitoes (Diagne et al., 2015), has been targeted with various antiviral strategies. Ribavirin has shown efficacy in suppressing viremia in ZIKV-infected STAT-1-deficient mice (Kamiyama et al., 2017), while favipiravir and BCX4430 inhibit viral RNA synthesis by targeting viral RNA-dependent RNA polymerase (Furuta et al., 2009; Eyer et al., 2017). The similarity between the envelope proteins of dengue and Zika viruses underscores their close evolutionary relationship (Lunardelli et al., 2023). NS1 protein plays critical roles in ZIKV replication (Valente and Moraes, 2019), and aptamer technology holds promise for enhancing antiviral drug efficacy by targeting specific virulence factors (Feng et al., 2011).

Nipah virus lacks specific antiviral treatments, making aptamer-based therapies a potential breakthrough by targeting its virulence factors, such as the F protein that mediates viral entry through ephrin B2/B3 receptors (Sun et al., 2018; Weis and Maisner, 2015). The Nipah virus V protein inhibits STAT proteins, crucial for interferon signaling, enhancing viral pathogenesis (Shaw et al., 2004). Aptamers designed to bind these proteins could mitigate infection severity.

Ebola virus VP35 and VP24 proteins are key virulence factors that disrupt host immune responses (Leung et al., 2010; Zhang et al.,

2012), with aptamers identified to target VP35's interferon inhibitory domain (Binning et al., 2013). These aptamers offer potential therapeutic avenues against Ebola virus by restoring interferon response pathways.

Influenza A viruses, characterized by their surface proteins HA and NA, play crucial roles in viral entry and replication (Bouvier and Palese, 2008). Aptamers targeting HA have demonstrated significant antiviral effects in animal models, inhibiting viral replication and reducing infection rates across different influenza strains (Nobusawa, 1997; Gopinath et al., 2006; Jeon et al., 2004). Aptamer research continues to explore novel therapeutic strategies, addressing the challenges posed by viral mutation and enhancing treatment efficacy (Musafia et al., 2014; Sanjuán, 2012).

5.2 Recent advancements and case studies

5.2.1 Notable developments in aptamer research for infectious diseases

5.2.1.1 Gold nanoparticle-DNA aptamer conjugate-assisted delivery of antimicrobial peptide (CA2634987A1)

Gold nanoparticles are a durable and widely used delivery technology that offers various benefits over liposomes and PLGA. It was demonstrated that combining antimicrobial peptides with a gold nanoparticle-aptamer complex was effective in eliminating intracellular Salmonella enterica serovar Typhimurium (Yeom et al., 2016).

TABLE 4 Therapeutic techniques and mechanisms of aptamers against the virus.

Virulence factors of Viruses					
S. No.	Virus	Virulence factor	Function	Mechanism	Reference
1	Zika	NS1 (non-structural protein 1)	Immune evasion and modulation	■ NS1 prevents the synthesis of interferon-beta (IFN-β), ■ Essential for the antiviral immune response.	(Rastogi and Singh, 2020)
		NS2A and NS4B	Viral replication	■ The Zika virus's NS2A contributes to the suppression of NF-κB promoter activity. ■ NS2A is composed of a central region (the bridge) that passes through a cellular compartment (ER) & six arms (segments) that extend outward from the central region.	(Lee et al., 2020) (Nutho et al., 2019)
		Envelope protein	Entry into host cell and helps in assembly of new viral particles	■ E protein promotes the production of viral particles by interacting with apolipoprotein E, a protein involved in lipid metabolism. ■ C-type lectin receptors in the host cell are involved in receptor-mediated endocytosis.	(Nutho et al., 2019) (Agrelli et al., 2019)
		Capsid protein	Helps in formation of new virus particles	■ capsid protein forms overall positively charged dimers that bridge RNA and lipid membrane surfaces. ■ The protein exists as dimers with four α helices and a long pre-α1 loop, contributing to its unique structure	(Shang et al., 2018)
2	Ebola	Viral protein 24 (VP24)	Interferes in host interferon and evades host immune system	■ VP24 suppresses interferon-dependent signaling, of interferon alpha/beta (IFN-α/β). ■ The host's antiviral response is interfered, which makes it easier for the virus to multiply and propagate.	(Zhang et al., 2012)
		VP30	Helps in transcription and replication	■ Dynamic phosphorylation of VP30 occurs at six serine residues at the N-terminus. ■ This post-translational alteration affects VP30's function in viral transcription and replication by regulating its activity in conjunction with dephosphorylation.	(Lier et al., 2017)
		VP35	Interferes with host interferon regulatory factor (IRFs)	■ VP35 interacts with the PKA-CREB1 pathway, a set of intracellular chemical signals. ■ A biological protein known as AKIP1 is bound by VP35, starting a chain reaction. ■ PKA (Protein Kinase A) and CREB1 (cAMP Response Element-Binding Protein 1), two important participants, are activated by this binding. ■ Following activation, CREB1 is drawn to viral inclusion bodies, which are particular structures created when the Ebola virus infects a host.	(Zhu et al., 2022)
		VP40	Formation and release of viral particles from infected cells	■ SUMOylation is a post-translational modification that controls VP40. ■ Affects the stability, nucleocapsid recruitment, structure, and budding of the virus.	(Baz-Martnez et al., 2016)
		L Polymerase	RNA dependent RNA polymerase involved in replication and transcription	■ The process includes the polymerase starting RNA synthesis from scratch, or de novo, without the aid of an existing primer.	(Yuan et al., 2022)
3	Nipah	Nucleoprotein (N protein)	responsible for enclosure of viral RNA genome	■ The N protein facilitates the interchange of N-terminal (NTARM) and C-terminal subdomains (CTARM) and lateral interactions that lead to the creation of a stable homopolymer structure.	(Ker et al., 2021)

(Continued)

TABLE 4 Continued

			Virulence factors of Viruses		
S. No.	Virus	Virulence factor	Function	Mechanism	Reference
				■ This particular structural configuration enhances the nucleocapsid's integrity.	
		Phosphoprotein (P protein)	Crucial for viral RNA synthesis and synthesis	■ Viral polymerase activity and viral RNA synthesis are regulated by overexpression of the Nipah virus nucleocapsid protein (N) ■ Which indicates the complex interaction between P and other viral components.	(Ranadheera et al., 2018)
		Matrix protein (M protein)	Involved in assembly and budding of new vial particles	■ The induction of interferon-beta (IFNβ) at the level of the TBK1/IKKε kinases is inhibited by the NiV matrix protein.	(Bharaj et al., 2016)
		Fusion protein (F protein)	Helps in viral entry into host cells	■ The attachment (G) protein and the NiV-F protein work together to mediate viral entry and syncytium formation. ■ Syncytium formation is the process by which adjacent and infected cells combine to promote the spread of the virus.	(Aguilar et al., 2006)
4	Influenza A virus	Hemagglutinin HA	Helps in adherence to host cell	■ Low pH inside endosomes causes HA to undergo a conformational shift after attachment. ■ The fusing of the viral and endosomal membranes can be mediated by HA ■ Conformational shift exposes a fusion peptide. ■ The viral genome must pass through this stage in order to enter the cytoplasm of the host cell.	(Brandenburg et al., 2013)
		Neuraminidase NA	Releases viral particles from infected cells	■ Neuraminidase is an exosialidase that breaks the α-ketosidic bond between the sugar residue next to the sialic acid on the surface of host cells that are infected. ■ The release of offspring viruses from the host cell membrane depends on this cleavage.	(McAuley et al., 2019)
		PB1, PB2, PA	Viral replication	■ The catalytic component responsible for RNA-dependent RNA polymerase (RdRP) activity is called PB1. ■ PB2 participates in the cap-snatching process, responsible for the start of viral transcription. To facilitate the production of viral mRNA, the viral polymerase snatches the 5' cap structure from host pre-mRNAs. ■ In the cap-snatching procedure, PA is an essential component. Sue to its endonuclease activity, host mRNA can be broken down close to the 5' cap structure. ■ Afterwards, PB2 uses this cleaved cap to start viral transcription.	(Binh et al., 2013) (Lerminiaux et al., 2020) (Ma et al., 2017)
		NP	Responsible for enclosure of viral RNA genome	■ The results show that NP serves a variety of purposes throughout the life cycle of the virus, and its requirement varies depending on the particular circumstances or context of the viral activities under investigation.	(Turrell et al., 2013)
		M1 M2	Involved in assembly and budding of new vial particles	■ M1's conformation may be affected by association with M2, which would promote the elongation of viral budding. ■ The effective release of new virus particles depends on this interaction.	(Roberts et al., 1998)
		NS1 NS2	Immune evasion	■ NS1 suppresses host's antiviral defenses by blocking several pathways, including interferon generation and activation of PKR	(Huang et al., 2017) (O'Neill et al., 1998)

(Continued)

TABLE 4 Continued

Virulence factors of Viruses					
S. No.	Virus	Virulence factor	Function	Mechanism	Reference
				(Protein Kinase R). ■ The nuclear export of viral ribonucleoprotein (vRNP) complexes is facilitated by NS2. ■ It controls the movement of NS2 mRNA that has been spliced and its precursor, NS1 mRNA, making it easier for vital viral components to be exported from the nucleus into the cytoplasm.	
5	Noro virus	VP1 (major capsule protein)	Formation of viral capsid, contributes to stability of virion	■ The capacity of the virus to reproduce in B cells is closely correlated with the projecting domain of VP1 ■ Potential function for this domain in determining norovirus virulence.	(Zhu et al., 2016)
		VP2 (minor structural protein)	Contributes for the stability of the virion	■ VP2 experiences coevolution and is the cause of most illnesses. Its significance in the infection process is shown by the coevolutionary dynamics.	(Hong et al., 2022)

5.2.1.2 Point-of-care SARS-CoV-2 salivary antigen testing with an off-the-shelf glucometer (WO2022016163A2)

An innovative test technique that combines a pre-conjugated aptamer with the enzyme invertase, which is then attached to a magnetic bead. Because the aptamer is highly specific to the antigen found in the corona virus, it goes through a confirmational change that releases the enzyme into the medium, where it is separated by magnetic separation. The medium's invertase then breaks down sucrose into glucose, and measuring the glucose yields an assay of the antigen present in the sample. This model operates on this concept (Singh et al., 2021).

5.2.1.3 Graphene aptasensor for the detection of hepatitis C virus (EP4124855A1)

Changes in their surroundings, particularly the attachment of bio-receptors to the graphene surface, cause Graphene Field-Effect Transistor Biosensors (gFET) to detect changes in electrical metrics, such as conductivity. Graphene's sensing potential is increased by chemical modification. As an example of how biological molecules can be sensed, researchers have created chemically functionalized gFETs that can detect negatively charged exosomes when they are bound to the graphene surface. In this particular case, researchers have created sgFETs with aptamer that can detect HCV protein even at lower concentrations making it an ultrasensitive aptasensor. Attomolar detection of the viral protein target is made possible by the enhanced sensitivity brought about by induced polarization at the graphene interface (Kwong Hong Tsang et al., 2019; Palacio et al., 2023).

5.2.1.4 Aptamer binding hemagglutinin of H7N7 subtype influenza virus (JP2014008002A)

An aptamer capable of differentiating between influenza A serotypes and interfering with the HA-glycan interaction was created by researchers. To ensure the aptamer's stability in the presence of endo-ribonucleases, 2′-fluoro cytidine is employed, which does not interfere with its binding to HA. This aptamer has applications in detecting and diagnosing H5N1 and H7N7 viruses, as well as in synthesizing virucidal drugs that selectively target these viruses, impeding their early interactions with hosts (Suenaga and Kumar, 2014). The glycoprotein known as hemaglutinin (HA), which is present on the influenza virus's surface, is essential to the virus's capacity to bind to and penetrate host cells. Aptamers work by specifically targeting HA, which stops the virus from attaching to host cell receptors and preventing it from entering the cells (Zou et al., 2019)

5.2.2 Case studies: aptamers that inhibit biofilm

Quorum sensing, a mechanism that enables signaling and communication within bacteria, plays a key role in the formation of *P.aeruginosa* biofilms. Three main QS systems in *P.aeruginosa*: *las* system, *rhl* system and *Pseudomonas quinolone signal* system (PQS) encode for various signaling molecules that act as regulator for the transcription of numerous virulence factor genes (Zhang et al., 2013; Chadha et al., 2022). Zhao et al., conducted a study in which they screened DNA aptamers complimentary to the signal molecule C4-HSL of the *rhl* system. Depressing the *rhl* system affects the formation and maintenance of the biofilm. It was observed that the biofilm formation of *P.aeruginosa* was efficiently reduced to about 1/3 by the aptamers compared with that of the groups without the aptamers in the *in vitro* biofilm inhibition experiments (Zhao et al., 2019) (Figure 4).

Matchawong et al., constructed a 2' -fluoropyrimidine modified nuclease-resistant RNA aptamersusing cell SELEX against *Streptococcus suis* serotype 2, strain P1/7. The R8-su12 RNA aptamer significantly reduced the *S. suis* biofilm formation and had the ability to bind to other pathogenic *S. suis* (serotype ½, 1, 9, and 14) (Matchawong et al., 2022). *Candida albicans* was grown in the exposure of condensed cigarette smoke (CSC), prepared from clove (CCSC) and non-clove (NCSC) cigarettes, for 48 h (Bachtiar et al., 2021).It was found that the presence of added CCSC or NCSC

significantly enhanced *C. albicans* biofilm development but when *C. albicans* was precoated with aptamer (Ca-apt1) there was a significant impairment in the biofilm development accelerated by the NCSC and CCSC. This could be attributed to the enhancement of the morphological changes of *C. albicans* (from yeast to hypha formation) due to CCSC or NCSC was reduced due to precoating the aptamer.

Ning et al.,conducted an interesting study in which a GO-loaded aptamer/berberine bifunctional complex specific to penicillin-binding protein 2a (PBP2a) significantly inhibited MRSA biofilm formation (Ning et al., 2022). The aptamer blocks the function of PBP2a, reducing surface-cell attachment and berberine attenuates the level of the accessory gene regulator (agr) system, which is essential for MRSA biofilm formation. Furthermore, GO also has the potential to disrupt cell membranes, attributing to the antibiofilm activity (Saravanan et al., 2023). Lijuan et al., developed an aptamer-ampicillin bifunctional conjugate that targeted bacterial flagella for treating biofilms (Lijuan et al., 2017).

6 Challenges and limitations

6.1 Stability and delivery concerns of aptamers

The term "steady state" describes the dynamic balance that results from consistent dosage between the total amount of a drug taken and its elimination. For aptamers, the steady-state or nearly steady-state concentration can be attained three to five times the half-life following aptamer administration, which has a steady-state duration of 17 to 29 hours (Lee et al., 2015). This emphasize on the importance of aptamer's stability i.e.,The longer the aptamer stays in circulation for the treatment of infectious disorders, the greater the likelihood that it may encounter pathogens. The pharmacokinetic profile of the aptamer must be determined to proceed with trials, firstly the aptamer's half-life *in vivo* is rather brief, lasting roughly 2 mins. Unmodified ssDNA oligonucleotides have a half-life of less than one minute (Griffin et al., 1993) (Sanjuán, 2012).

In conditioned media, HEK cells infected with *M. fermentans* exhibit ribonuclease activity that rapidly degrades RNA carrying 2′-fluoro- and 2′-O-methyl-modified pyrimidines. Similar ribonuclease activity was seen in a pure culture of *M.fermentans*, but not in a culture of uncontaminated HEK cells (Hernandez et al., 2012). RA-36, an aptamer with antithrombin properties, have shown rapid bloodstream elimination with a half life of 1 minute As opposed to 23 minutes in tissues (Zavyalova et al., 2017). The tissue type, aptamer sequence, and their formulation affects the outcomes of aptamer uptake ad distribution. A single bolus oral dose of aptamer was administered to mice, and after tissue contamination was eliminated with perfusion buffer, the aptamer was diffused into the bloodstream from the peritoneum and into multiple organs, including the brain and spinal cord, within minutes of oral administration. The uptake of the aptamer was reduced within a few hours (Perschbacher et al., 2015). When aptamer and nanoparticles are conjugated, the physiochemical properties including the size and distribution of the particles are altered (Ghassami et al., 2018).
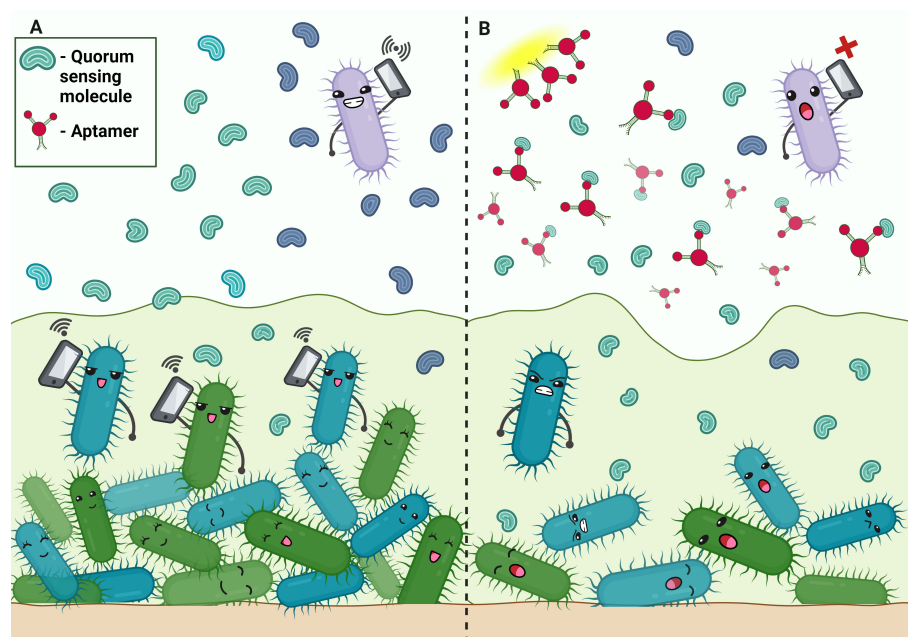

FIGURE 4
Aptamers disrupting quorum sensing in biofilm. **(A)** Communication in bacterial biofilm by quorum sensing molecule. **(B)** Aptamer binds to the quorum-sensing molecules, disrupting signaling.

6.2 Potential for off-target effects and safety issues

Drugs undergoing clinical trials may have side effects and safety problems of their own, but it is crucial to understand these effects in order to design a therapeutic version with less side effects. Investigations' findings by Zhao et.al., in the tested settings, the SGC8 aptamer exhibited neither mutagenicity nor genetic toxicity using total body-positron emitting tomography (TB PET) (D. Ding et al., 2023). When an aptamer-tagged radioactive element was injected intravenously, the kidney contained the highest quantities of radioactivity. This indicates that the pharmacokinetics profile of absorption from intravenous aptamer injection results in a relatively low absorption rate. However, giving aptamer was administered in many doses, but this did not cause aptamer to accumulate in plasma. The factor most likely limiting the drug's rate of disposal is its rate of absorption (Siddiqui and Keating, 2005).

Researchers discovered that the absence of conjugating cholesterol has certain undesirable effects, such as altering the expression of genes associated to innate immunity and cellular survival (Lee et al., 2015). In addition, the aptamer's overall negative charge causes it to attach to positively charged substances without being specific. As stated previously, the aptamer's short length and compact size promote bio clearance (Gholikhani et al., 2022).

6.3 Strategies to overcome challenges and ongoing research in the field

The aforementioned problems can be solved in a number of ways, and some of these tactics are (1) substituting sulfur for one of the monothio or dithio groups of the phosphoryl non-bridging oxygen atoms results in a number of benefits, including increased binding to the target, resistance to nuclease action, and faster absorption into the cells. However, there is a small drawback to this the aptamer may become less specific (Thiviyanathan et al., 2007; Keefe et al., 2010). (2) integrating aptamer into a larger molecular framework in the shape of a multivalent circle by offering nucleolytic stabilization that guards against exonucleases (Di Giusto et al., 2006). (3) the body's nuclease enzymes could not break down aptamers synthesized with an L nucleotide sequence. This type of sequence, called spigelmers, is the mirror image of an oligonucleotide but contains L nucleotide instead of R nucleotide (Maasch et al., 2008; Chen et al., 2017). (4) RNA sequences that have aldehyde derivatives appended to the 5' end, facilitate affinity purification and coupling with other molecules (Pfander et al., 2007). (5) producing the most stable hybrids by employing nucleoside analogues that have a methylene bond between the ribose ring's 2′-O and 4′-C in order to create a locked nucleic acid sequence. The sugar moiety is thus locked in a C3′-endo configuration (Lebars et al., 2007). (6) an aptamer was modified by adding PEG linkers to decrease stearic hinderance and 2'-fluoro-pyrimidines (2'F) (Derbyshire et al., 2012; Ni et al., 2021). (7) the highest tissue exposure was achieved by the aptamer, which was prepared as a 3′ biotin derivative coupled with tetrameric streptavidin (Perschbacher et al., 2015). To achieve this, a cholesterol moiety was linked to the 5' end of a 29-nucleotide RNA aptamer that had been modified with 2'-F against the HCV NS5B protein. This modification was chosen because previous studies have shown that conjugating oligonucleotide molecules with cholesterol can prolong their plasma half-life by associating with plasma lipoproteins and enhance their uptake by hepatic cells through receptor-mediated endocytosis. (8) An improved aptamer half-life results by conjugating cholesterol with the aptamer (Lee et al., 2015). (9) The aptamer attached to MetCyc, facilitating its interaction with other molecules helping evade attacks from nucleases (Borbas et al., 2007; Ni et al., 2021). (10) In some circumstances, we can employ liposomal conjugated aptamers to lengthen the drug's half-life and make it more covert (Jiang et al., 2020; Alameh et al., 2021; Kim et al., 2001). (11) To shield the RNA from exonuclease degradation, the derivative's two terminals are capped with an extended stem structure, allowing for the effective *in vivo* expression of the aptamer (Mori et al., 2012). Creating chimeric aptamers by combining segments from different aptamers or combining with other functional molecules for enhancing specificity (Cheng et al., 2023). In conclusion, these diverse strategies and modifications illustrate ongoing efforts to optimize aptamer technology, enhancing their stability, specificity, and therapeutic efficacy across various biomedical applications.

7 Conclusion and future perspectives

The diverse applications of aptamers in the realm of infectious diseases underscore their immense potential in diagnostics, therapeutics, and biosensing. The ability of aptamers to specifically recognize and bind to a wide range of pathogenic targets, including viruses, bacteria, and fungus, has paved the way for innovative solutions in disease detection and treatment. In diagnostics, aptamers have demonstrated exceptional sensitivity and specificity, enabling the development of rapid and accurate diagnostic assays. Their incorporation into biosensors has facilitated the detection of infectious agents at early stages, contributing to timely interventions and improved patient outcomes. Aptamer-based diagnostic platforms also offer the advantage of portability and cost-effectiveness, making them particularly valuable in resource-limited settings. Aptamers have proven their mettle in therapeutic applications, where they can be engineered to inhibit viral entry, replication, or modulate the host immune response. The versatility of aptamers allows for the design of tailored therapeutic interventions, offering a promising avenue for the development of antiviral and antibacterial agents. Moreover, the potential for aptamers to mitigate the emergence of drug-resistant strains adds another layer of significance to their therapeutic applications. Looking ahead, the future perspectives of aptamer research in infectious diseases are exciting and multifaceted. Advancements in aptamer selection technologies, such as SELEX, will likely enhance the discovery of aptamers with improved binding affinities and specificities. The integration of aptamers with emerging technologies, such as CRISPR-based diagnostics and gene editing, holds promise for the development of next-generation diagnostic and

therapeutic tools. Furthermore, the exploration of aptamer-nanoparticle conjugates and other delivery systems may enhance the targeted delivery of aptamers to infected tissues, improving their therapeutic efficacy. Collaborations between academia, industry, and healthcare providers will be crucial in translating aptamer-based technologies from the laboratory to clinical practice.

Author contributions

RN: Data curation, Visualization, Writing – original draft. BS: Visualization, Writing – original draft, Conceptualization. SS: Data curation, Visualization, Writing – original draft. AS: Data curation, Visualization, Writing – review & editing. SR: Data curation, Visualization, Writing – review & editing. HD: Conceptualization, Data curation, Supervision, Visualization, Writing – review & editing. AS: Conceptualization, Data curation, Supervision, Visualization, Writing – review & editing.

Funding

Acknowledgments

Conflict of interest

The authors declare that the research was conducted in the absence of any commercial or financial relationships that could be construed as a potential conflict of interest.

The author(s) declared that they were an editorial board member of Frontiers, at the time of submission. This had no impact on the peer review process and the final decision

Publisher's note

References

Adachi, T., and Nakamura, Y. (2019). Aptamers: A review of their chemical properties and modifications for therapeutic application. *Molecules* 24, 4229. doi: 10.3390/molecules24234229

Afrasiabi, S., Pourhajibagher, M., Raoofian, R., Tabarzad, M., and Bahador, A. (2020). Therapeutic applications of nucleic acid aptamers in microbial infections. *J. Biomed. Sci.* 27, 6. doi: 10.1186/s12929-019-0611-0

Agrelli, A., de Moura, R. R., Crovella, S., and Brandão, L. A. C. (2019). ZIKA virus entry mechanisms in human cells. *Infection Genet. Evol.* 69, 22–29. doi: 10.1016/j.meegid.2019.01.018

Aguilar, H. C., Matreyek, K. A., Filone, C. M., Hashimi, S. T., Levroney, E. L., Negrete, O. A., et al. (2006). N-Glycans on Nipah Virus fusion protein protect against neutralization but reduce membrane fusion and viral entry. *J. Virol.* 80, 4878–4889. doi: 10.1128/jvi.80.10.4878-4889.2006

Alameh, M.-G., Tombácz, I., Bettini, E., Lederer, K., Ndeupen, S., Sittplangkoon, C., et al. (2021). Lipid nanoparticles enhance the efficacy of mRNA and protein subunit vaccines by inducing robust T follicular helper cell and humoral responses. *Immunity* 54, 2877–2892.e7. doi: 10.1016/j.immuni.2021.11.001

Ali, M. H., Elsherbiny, M. E., and Emara, M. (2019). Updates on aptamer research. *Int. J. Mol. Sci.* 20, 2511. doi: 10.3390/ijms20102511

Aljohani, M. M., Cialla-May, D., Popp, J., Chinnappan, R., Al-Kattan, K., and Zourob, M. (2022). Aptamers: potential diagnostic and therapeutic agents for blood diseases. *Molecules* 27, 383. doi: 10.3390/molecules27020383

Almeida, N. B. F., Sousa, T. A. S. L., Santos, V. C. F., Lacerda, C. M. S., Silva, T. G., Grenfell, R. F. Q., et al. (2022). DNA aptamer selection and construction of an aptasensor based on graphene FETs for Zika virus NS1 protein detection. *Beilstein J. Nanotechnology* 13, 873–881. doi: 10.3762/bjnano.13.78

Amouzadeh Tabrizi, M., and Acedo, P. (2022). Highly sensitive aptasensor for the detection of SARS-CoV-2-RBD using aptamer-gated methylene blue@mesoporous silica film/laser engraved graphene electrode. *Biosensors Bioelectronics* 215, 114556. doi: 10.1016/j.bios.2022.114556

A Ocsoy, M., Yusufbeyoglu, S., Ildiz, N., Ulgen, A., and Ocsoy, I. (2021). DNA aptamer-conjugated magnetic graphene oxide for pathogenic bacteria aggregation: selective and enhanced photothermal therapy for effective and rapid killing. *ACS Omega* 6, 20637–20643. doi: 10.1021/acsomega.1c02832

Askari, A., Kota, S., Ferrell, H., Swamy, S., Goodman, K. S., Okoro, C. C., et al. (2024). UTexas Aptamer Database: the collection and long-term preservation of aptamer sequence information. *Nucleic Acids Res.* 52, D351–D359. doi: 10.1093/nar/gkad959

Aslan, Y., Atabay, M., Chowdhury, H. K., Göktürk, I., Saylan, Y., and Inci, F. (2023). Aptamer-based point-of-care devices: emerging technologies and integration of computational methods. *Biosensors* 13, 569. doi: 10.3390/bios13050569

Augenstreich, J., Haanappel, E., Sayes, F., Simeone, R., Guillet, V., Mazeres, S., et al. (2020). Phthiocerol dimycocerosates from *Mycobacterium tuberculosis* increase the membrane activity of bacterial effectors and host receptors. *Front. Cell. Infection Microbiol.* 10. doi: 10.3389/fcimb.2020.00420

Bachour Junior, B., Batistuti, M. R., Pereira, A. S., de Sousa Russo, E. M., and Mulato, M. (2021). Electrochemical aptasensor for NS1 detection: Towards a fast dengue biosensor. *Talanta* 233, 122527. doi: 10.1016/j.talanta.2021.122527

Bachtiar, B. M., Gani, B. A., Deviana, A., Utami, N. R., Andriyani, A. D., and Bachtiar, E. W. (2021). The discrepancy between clove and non-clove cigarette smoke-promoted *Candida albicans* biofilm formation with precoating RNA-aptamer. *F1000Research* 10, 372. doi: 10.12688/f1000research.52266.3

Bagheri Pebdeni, A., Mousavizadegan, M., and Hosseini, M. (2021). Sensitive detection of S. aureus using aptamer- and vancomycin -copper nanoclusters as dual recognition strategy. *Food Chem.* 361, 130137. doi: 10.1016/j.foodchem.2021.130137

Bagheryan, Z., Raoof, J.-B., Golabi, M., Turner, A. P. F., and Beni, V. (2016). Diazonium-based impedimetric aptasensor for the rapid label-free detection of *Salmonella typhimurium* in food sample. *Biosensors Bioelectronics* 80, 566–573. doi: 10.1016/j.bios.2016.02.024

Bai, X., Nakatsu, C. H., and Bhunia, A. K. (2021). Bacterial biofilms and their implications in pathogenesis and food safety. *Foods* 10, 2117. doi: 10.3390/foods10092117

Bakhtiari, H., Palizban, A. A., Khanahmad, H., and Mofid, M. R. (2021). Novel approach to overcome defects of Cell-SELEX in developing aptamers against aspartate β-hydroxylase. *ACS Omega* 6, 11005–11014. doi: 10.1021/acsomega.1c00876

Bayraç, A. T., and Donmez, S. I. (2018). Selection of DNA aptamers to *Streptococcus pneumonia* and fabrication of graphene oxide based fluorescent assay. *Analytical Biochem.* 556, 91–98. doi: 10.1016/j.ab.2018.06.024

Baz-Martnez, M., El Motiam, A., Ruibal, P., Condezo, G. N., de la Cruz-Herrera, C. F., Lang, V., et al. (2016). Regulation of Ebola virus VP40 matrix protein by SUMO. *Sci. Rep.* 6. doi: 10.1038/srep37258

Bell, R. L., Jarvis, K. G., Ottesen, A. R., McFarland, M. A., and Brown, E. W. (2016). Recent and emerging innovations in *Salmonella* detection: a food and environmental perspective. *Microbial Biotechnol.* 9, 279–292. doi: 10.1111/1751-7915.12359

Bharaj, P., Wang, Y. E., Dawes, B. E., Yun, T. E., Park, A., Yen, B., et al. (2016). The matrix protein of nipah virus targets the E3-ubiquitin ligase TRIM6 to inhibit the IKKε kinase-mediated type-I IFN antiviral response. *PLoS Pathog.* 12. doi: 10.1371/journal.ppat.1005880

Binh, N. T., Wakai, C., Kawaguchi, A., and Nagata, K. (2013). The N-terminal region of influenza virus polymerase PB1 adjacent to the PA binding site is involved in replication but not transcription of the viral genome. *Front. Microbiol.* 4. doi: 10.3389/fmicb.2013.00398

Binning, J. M., Wang, T., Luthra, P., Shabman, R. S., Borek, D. M., Liu, G., et al. (2013). Development of RNA aptamers targeting ebola virus VP35. *Biochemistry* 52, 8406–8419. doi: 10.1021/bi400704d

Borbas, K. E., Ferreira, C. S. M., Perkins, A., Bruce, J. I., and Missailidis, S. (2007). design and synthesis of mono- and multimeric targeted radiopharmaceuticals based on novel cyclen ligands coupled to Anti-MUC1 aptamers for the diagnostic imaging and targeted radiotherapy of cancer. *Bioconjugate Chem.* 18, 1205–1212. doi: 10.1021/bc0700741

Boussebayle, A., Groher, F., and Suess, B. (2019). RNA-based Capture-SELEX for the selection of small molecule-binding aptamers. *Methods* 161, 10–15. doi: 10.1016/j.ymeth.2019.04.004

Bouvier, N. M., and Palese, P. (2008). The biology of influenza viruses. *Vaccine* 26, D49–D53. doi: 10.1016/j.vaccine.2008.07.039

Brandenburg, B., Koudstaal, W., Goudsmit, J., Klaren, V., Tang, C., Bujny, M. V., et al. (2013). Mechanisms of hemagglutinin targeted influenza virus neutralization. *PLoS One* 8 (12), e80034. doi: 10.1371/journal.pone.0080034

Brody, E., Willis, M., Smith, J., Jayasena, S., Zichi, D., and Gold, L. (1999). The use of aptamers in large arrays for molecular diagnostics. *Mol. Diagnosis* 4, 381–388. doi: 10.1016/S1084-8592(99)80014-9

Brooks, L. R. K., and Mias, G. I. (2018). *Streptococcus pneumoniae*'s virulence and host immunity: Aging, diagnostics, and prevention. *Front. Immunol.* 9. doi: 10.3389/fimmu.2018.01366

Brosel-Oliu, S., Ferreira, R., Uria, N., Abramova, N., Gargallo, R., Muñoz-Pascual, F.-X., et al. (2018). Novel impedimetric aptasensor for label-free detection of *Escherichia coli* O157:H7. *Sensors Actuators B: Chem.* 255, 2988–2995. doi: 10.1016/j.snb.2017.09.121

Brosseau, N. E., Vallée, I., Mayer-Scholl, A., Ndao, M., and Karadjian, G. (2023). Aptamer-based technologies for parasite detection. *Sensors* 23, 562. doi: 10.3390/s23020562

Canova, M. J., and Molle, V. (2014). Bacterial serine/threonine protein kinases in host-pathogen interactions. *J. Biol. Chem.* 289, 9473–9479). doi: 10.1074/jbc.R113.529917

Capatina, D., Lupoi, T., Feier, B., Blidar, A., Hosu, O., Tertis, M., et al. (2022). Label-free electrochemical aptasensor for the detection of the 3-O-C12-HSL quorum-sensing molecule in *Pseudomonas aeruginosa. Biosensors* 12, 440. doi: 10.3390/bios12070440

Chadha, J., Harjai, K., and Chhibber, S. (2022). Revisiting the virulence hallmarks of Pseudomonas aeruginosa : a chronicle through the perspective of quorum sensing. *Environ. Microbiol.* 24, 2630–2656. doi: 10.1111/1462-2920.15784

Chauhan, P., Datta, I., Dhiman, A., Shankar, U., Kumar, A., Vashist, A., et al. (2022). DNA aptamer targets *Mycobacterium tuberculosis* DevR/DosR response regulator function by inhibiting its dimerization and DNA binding activity. *ACS Infect. Dis.* 8, 2540–2551. doi: 10.1021/acsinfecdis.2c00414

Chen, X., Chang, Y., Ye, M., Wang, Z., Wu, S., and Duan, N. (2024). Rational design of a robust g-quadruplex aptamer as an inhibitor to alleviate *Listeria monocytogenes* infection. *ACS Appl. Materials Interfaces* 16, 15946–15958. doi: 10.1021/acsami.4c00496

Chen, W., Cui, L., Song, Y., Chen, W., Su, Y., Chang, W., et al. (2021b). Detection of Listeria monocytogenes using luminol-functionalized AuNF-Labeled aptamer recognition and magnetic separation. *ACS Omega* 6, 26338–26344. doi: 10.1021/acsomega.1c03527

Chen, Z., Luo, H., Gubu, A., Yu, S., Zhang, H., Dai, H., et al. (2023). Chemically modified aptamers for improving binding affinity to the target proteins via enhanced non-covalent bonding. *Front. Cell Dev. Biol.* 11, 1091809. doi: 10.3389/fcell.2023.1091809

Chen, X., Ma, Y., Xie, Y., and Pu, J. (2022a). Aptamer-based applications for cardiovascular disease. *Front. Bioengineering Biotechnol.* 10. doi: 10.3389/fbioe.2022.1002285

Chen, H., Park, S.-G., Choi, N., Moon, J.-I., Dang, H., Das, A., et al. (2020). SERS imaging-based aptasensor for ultrasensitive and reproducible detection of influenza virus A. *Biosensors Bioelectronics* 167, 112496. doi: 10.1016/j.bios.2020.112496

Chen, W., Wu, J., Li, S., Zhang, H., Cui, L., Liu, J., et al. (2021c). Ultrasensitive detection of Listeria monocytogenes using solid-state electrochemiluminescence biosensing based on the quenching effect of ferrocene on ruthenium pyridine. *J. Food Saf.* 41. doi: 10.1111/jfs.12868

Chen, H., Xie, S., Liang, H., Wu, C., Cui, L., Huan, S.-Y., et al. (2017). Generation of biostable L-aptamers against achiral targets by chiral inversion of existing D-aptamers. *Talanta* 164, 662–667. doi: 10.1016/j.talanta.2016.11.001

Chen, M., Yu, Y., Jiang, F., Zhou, J., Li, Y., Liang, C., et al. (2016). Development of Cell-SELEX technology and its application in cancer diagnosis and therapy. *Int. J. Mol. Sci.* 17, 2079. doi: 10.3390/ijms17122079

Chen, X.-F., Zhao, X., and Yang, Z. (2022b). Aptasensors for the detection of infectious pathogens: design strategies and point-of-care testing. *Microchimica Acta* 189, 443. doi: 10.1007/s00604-022-05533-w

Chen, S., Zong, X., Zheng, J., Zhang, J., Zhou, M., Chen, Q., et al. (2021a). A colorimetric strategy based on aptamer-catalyzed hairpin assembly for the on-site detection of salmonella typhimurium in milk. *Foods* 10 (11), 2539. doi: 10.3390/foods10112539

Chessa, D., Spiga, L., de Riu, N., Delaconi, P., Mazzarello, V., Ganau, G., et al. (2014). Lipopolysaccharides belonging to different Salmonella serovars are differentially capable of activating toll-like receptor 4. *Infection Immun.* 82, 4553–4562. doi: 10.1128/IAI.02297-14

Cohen, M. L. (2000). Changing patterns of infectious disease. *Nature* 406, 762–767. doi: 10.1038/35021206

Dai, G., Li, Y., Li, Z., Zhang, J., Geng, X., Zhang, F., et al. (2022). Zirconium-based metal–organic framework and Ti3C2Tx nanosheet-based faraday cage-type electrochemical aptasensor for Escherichia coli detection. *ACS Appl. Nano Materials* 5, 9201–9208. doi: 10.1021/acsanm.2c01548

Damborský, P., Švitel, J., and Katrlík, J. (2016). Optical biosensors. *Essays Biochem.* 60, 91–100. doi: 10.1042/EBC20150010

Derbyshire, N., White, S. J., Bunka, D. H. J., Song, L., Stead, S., Tarbin, J., et al. (2012). Toggled RNA aptamers against aminoglycosides allowing facile detection of antibiotics using gold nanoparticle assays. *Analytical Chem.* 84, 6595–6602. doi: 10.1021/ac300815c

Dhiman, A., Kumar, C., Mishra, S. K., Sikri, K., Datta, I., Sharma, P., et al. (2019). Theranostic application of a novel G-quadruplex-forming DNA aptamer targeting malate synthase of Mycobacterium tuberculosis. *Mol. Ther. Nucleic Acids* 18, 661–672. doi: 10.1016/j.omtn.2019.09.026

Diagne, C. T., Diallo, D., Faye, O., Ba, Y., Faye, O., Gaye, A., et al. (2015). Potential of selected Senegalese Aedes spp. mosquitoes (Diptera: Culicidae) to transmit Zika virus. *BMC Infect. Dis.* 15, 492. doi: 10.1186/s12879-015-1231-2

Di Giusto, D. A., Knox, S. M., Lai, Y., Tyrelle, G. D., Aung, M. T., and King, G. C. (2006). Multitasking by multivalent circular DNA aptamers. *ChemBioChem* 7, 535–544. doi: 10.1002/cbic.200500316

Ding, Y., and Liu, J. (2023). Quantitative comparison of Capture-SELEX, GO-SELEX, and Gold-SELEX for enrichment of aptamers. *Analytical Chem.* 95, 14651–14658. doi: 10.1021/acs.analchem.3c02477

Ding, D., Zhao, H., Wei, D., Yang, Q., Yang, C., Wang, R., et al. (2023). The first-in-human whole-body dynamic pharmacokinetics study of aptamer. *Research* 6. doi: 10.34133/research.0126

Doherty, M. K., Shaw, C., Woods, L., and Weimer, B. C. (2023). Alpha-gal bound aptamer and vancomycin synergistically reduce *Staphylococcus aureus* infection In vivo. *Microorganisms* 11 (7), 1776. doi: 10.3390/microorganisms11071776

Dong, Y., Wang, Z., Wang, S., Wu, Y., Ma, Y., and Liu, J. (2018). "Introduction of SELEX and important SELEX variants," in *Aptamers for Analytical Applications: Affinity Acquisition and Method Design*, pp.1–pp25.

Dramsi, S., and Cossart, P. (2002). Listeriolysin O. *J. Cell Biol.* 156, 943–946. doi: 10.1083/jcb.200202121

Du, J., Chen, X., Liu, K., Zhao, D., and Bai, Y. (2022). Dual recognition and highly sensitive detection of *Listeria monocytogenes* in food by fluorescence enhancement effect based on Fe3O4@ZIF-8-aptamer. *Sensors Actuators B: Chem.* 360, 131654. doi: 10.1016/j.snb.2022.131654

Duan, N., Chang, B., Zhang, H., Wang, Z., and Wu, S. (2016). Salmonella typhimurium detection using a surface-enhanced Raman scattering-based aptasensor. *Int. J. Food Microbiol.* 218, 38–43. doi: 10.1016/j.ijfoodmicro.2015.11.006

Duan, N., Wu, S., Zhu, C., Ma, X., Wang, Z., Yu, Y., et al. (2012). Dual-color upconversion fluorescence and aptamer-functionalized magnetic nanoparticles-based bioassay for the simultaneous detection of *Salmonella Typhimurium* and *Staphylococcus aureus. Analytica Chimica Acta* 723, 1–6. doi: 10.1016/j.aca.2012.02.011

El-Wekil, M. M., Halby, H. M., Darweesh, M., Ali, M. E., and Ali, R. (2022). An innovative dual recognition aptasensor for specific detection of *Staphylococcus aureus* based on Au/Fe3O4 binary hybrid. *Sci. Rep.* 12, 12502. doi: 10.1038/s41598-022-15637-1

Escolano, J. M., Díaz-Durán, B., DeMiguel-Ramos, M., Olivares, J., Geday, M. A., and Iborra, E. (2017). Selection of aptamers to *Neisseria meningitidis* and *Streptococcus pneumoniae* surface specific proteins and affinity assay using thin film AlN resonators. *Sensors Actuators B: Chem.* 246, 591–596. doi: 10.1016/j.snb.2017.02.098

Eyer, L., Zouharová, D., Širmarová, J., Fojtíková, M., Štefánik, M., Haviernik, J., et al. (2017). Antiviral activity of the adenosine analogue BCX4430 against West Nile virus and tick-borne flaviviruses. *Antiviral Res.* 142, 63–67. doi: 10.1016/j.antiviral.2017.03.012

Fair, R. J., and Tor, Y. (2014). Antibiotics and bacterial resistance in the 21st century. *Perspect. Medicinal Chem.* 6, PMC.S14459. doi: 10.4137/PMC.S14459

Fang, S., Song, D., Zhuo, Y., Chen, Y., Zhu, A., and Long, F. (2021). Simultaneous and sensitive determination of *Escherichia coli* O157:H7 and *Salmonella typhimurium* using evanescent wave dual-color fluorescence aptasensor based on micro/nano size effect. *Biosensors Bioelectronics* 185, 113288. doi: 10.1016/j.bios.2021.113288

Fathi, S., Saber, R., Adabi, M., Rasouli, R., Douraghi, M., Morshedi, M., et al. (2020). Novel competitive voltammetric aptasensor based on electrospun carbon nanofibers-gold nanoparticles modified graphite electrode for salmonella enterica serovar

detection. *Biointerface Res. Appl. Chem.* 11, 8702–8715. doi: 10.33263/BRIAC112.87028715

Faucher, S. P., Viau, C., Gros, P. P., Daigle, F., and Le Moual, H. (2008). The prpZ gene cluster encoding eukaryotic-type Ser/Thr protein kinases and phosphatases is repressed by oxidative stress and involved in *Salmonella enterica* serovar Typhi survival in human macrophages. *FEMS Microbiol. Lett.* 281, 160–166. doi: 10.1111/j.1574-6968.2008.01094.x

Feng, H., Beck, J., Nassal, M., and Hu, K. (2011). A SELEX-Screened aptamer of human hepatitis B virus RNA encapsidation signal suppresses viral replication. *PLoS One* 6, e27862. doi: 10.1371/journal.pone.0027862

Ferhan, A. R., Jackman, J. A., and Cho, N.-J. (2016). Integration of quartz crystal microbalance-dissipation and reflection-mode localized surface plasmon resonance sensors for biomacromolecular interaction analysis. *Analytical Chem.* 88, 12524–12531. doi: 10.1021/acs.analchem.6b04303

Fowler, C. C., and Galán, J. E. (2018). Decoding a *Salmonella typhi* regulatory network that controls typhoid toxin expression within human cells. *Cell Host Microbe* 23, 65–76.e6. doi: 10.1016/j.chom.2017.12.001

Furuta, Y., Takahashi, K., Shiraki, K., Sakamoto, K., Smee, D. F., Barnard, D. L., et al. (2009). T-705 (favipiravir) and related compounds: Novel broad-spectrum inhibitors of RNA viral infections. *Antiviral Res.* 82, 95–102. doi: 10.1016/j.antiviral.2009.02.198

Galán, J. E. (2016). Typhoid toxin provides a window into typhoid fever and the biology of Salmonella Typhi. *Proc. Natl. Acad. Sci.* 113, 6338–6344. doi: 10.1073/pnas.1606335113

Gao, R., Zhong, Z., Gao, X., and Jia, L. (2018). Graphene oxide quantum dots assisted construction of fluorescent aptasensor for rapid detection of *Pseudomonas aeruginosa* in food samples. *J. Agric. Food Chem.* 66, 10898–10905. doi: 10.1021/acs.jafc.8b02164

García-Recio, E. M., Pinto-Díez, C., Pérez-Morgado, M. I., García-Hernández, M., Fernández, G., Martín, M. E., et al. (2016). Characterization of MNK1b DNA Aptamers that inhibit proliferation in MDA-MB231 breast cancer cells. *Mol. Ther. - Nucleic Acids* 5, e275. doi: 10.1038/mtna.2015.50

Ge, C., Feng, J., Zhang, J., Hu, K., Wang, D., Zha, L., et al. (2022). Aptamer/antibody sandwich method for digital detection of SARS-CoV2 nucleocapsid protein. *Talanta* 236, 122847. doi: 10.1016/j.talanta.2021.122847

Gerlach, R. G., Jäckel, D., Stecher, B., Wagner, C., Lupas, A., Hardt, W. D., et al. (2007). Salmonella Pathogenicity Island 4 encodes a giant non-fimbrial adhesin and the cognate type 1 secretion system. *Cell. Microbiol.* 9, 1834–1850. doi: 10.1111/j.1462-5822.2007.00919.x

Ghassami, E., Varshosaz, J., Jahanian-Najafabadi, A., Minaiyan, M., Rajabi, P., and Hayati, E. (2018). Pharmacokinetics and *in vitro/in vivo* antitumor efficacy of aptamer-targeted Ecoflex® nanoparticles for docetaxel delivery in ovarian cancer. *Int. J. Nanomedicine Volume* 13, 493–504. doi: 10.2147/IJN.S152474

Gholikhani, T., Kumar, S., Valizadeh, H., Mahdinloo, S., Adibkia, K., Zakeri-Milani, P., et al. (2022). Advances in aptamers-based applications in breast cancer: drug delivery, therapeutics, and diagnostics. *Int. J. Mol. Sci.* 23, 14475. doi: 10.3390/ijms232214475

Gopinath, S. C. B. (2007). Methods developed for SELEX. *Analytical Bioanalytical Chem.* 387, 171–182. doi: 10.1007/s00216-006-0826-2

Gopinath, S. C. B., Misono, T. S., Kawasaki, K., Mizuno, T., Imai, M., Odagiri, T., et al. (2006). An RNA aptamer that distinguishes between closely related human influenza viruses and inhibits haemagglutinin-mediated membrane fusion. *J. Gen. Virol.* 87, 479–487. doi: 10.1099/vir.0.81508-0

Gribanyov, D., Zhdanov, G., Olenin, A., Lisichkin, G., Gambaryan, A., Kukushkin, V., et al. (2021). SERS-Based colloidal aptasensors for quantitative determination of influenza virus. *Int. J. Mol. Sci.* 22, 1842. doi: 10.3390/ijms22041842

Griffin, L., Tidmarsh, G., Bock, L., Toole, J., and Leung, L. (1993). *In vivo* anticoagulant properties of a novel nucleotide-based thrombin inhibitor and demonstration of regional anticoagulation in extracorporeal circuits. *Blood* 81, 3271–3276. doi: 10.1182/blood.V81.12.3271.3271

Gründling, A., Burrack, L. S., Bouwer, H. A., and Higgins, D. E. (2004). *Listeria monocytogenes* regulates flagellar motility gene expression through MogR, a transcriptional repressor required for virulence. *Proc Natl Acad Sci.* 101 (33), 12318–12323.

Hamedani, N. S., and Müller, J. (2016). Capillary electrophoresis for the selection of DNA aptamers recognizing activated protein C. *Nucleic acid aptamers: selection, characterization, and application.* 1380, 61–75. doi: 10.1007/978-1-4939-3197-2_5

Hameed, S. S., Al-Ogaili, A. S., and Noori, N. (2022). Single-stranded DNA aptamer-based rolling circle amplification as anti-chicken *Salmonella* bacteriostatic. *Veterinary World* 15, 1171–1176. doi: 10.14202/vetworld.2022.1171-1176

Hernandez, F. J., Stockdale, K. R., Huang, L., Horswill, A. R., Behlke, M. A., and McNamara, J. O. (2012). Degradation of nuclease-stabilized RNA oligonucleotides in mycoplasma-contaminated cell culture media. *Nucleic Acid Ther.* 22, 58–68. doi: 10.1089/nat.2011.0316

Hong, X., Xue, L., Gao, J., Jiang, Y., and Kou, X. (2022). Epochal coevolution of minor capsid protein in norovirus GII.4 variants with major capsid protein based on their interactions over the last five decades. *Virus Res.* 319, 198860. doi: 10.1016/j.virusres.2022.198860

Huang, X., Zheng, M., Wang, P., Mok, B. W. Y., Liu, S., Lau, S. Y., et al. (2017). An NS-segment exonic splicing enhancer regulates influenza A virus replication in mammalian cells. *Nat. Commun.* 8 (1), 14751. doi: 10.1038/ncomms14751

Hui, Y., Peng, H., Zhang, F., Zhang, L., Liu, Y., Jia, R., et al. (2022). An ultrasensitive sandwich-type electrochemical aptasensor using silver nanoparticle/titanium carbide nanocomposites for the determination of *Staphylococcus aureus* in milk. *Microchimica Acta* 189, 276. doi: 10.1007/s00604-022-05349-8

Jeon, S. H., Kayhan, B., Ben-Yedidia, T., and Arnon, R. (2004). A DNA aptamer prevents influenza infection by blocking the receptor binding region of the viral hemagglutinin. *J. Biol. Chem.* 279, 48410–48419. doi: 10.1074/jbc.M409059200

Jia, F., Bai, X., Zhang, X., Fu, Y., Li, Y., Li, X., et al. (2021). A low-field magnetic resonance imaging aptasensor for the rapid and visual sensing of *Pseudomonas aeruginosa* in food, juice, and water. *Analytical Chem.* 93, 8631–8637. doi: 10.1021/acs.analchem.1c01669

Jia, F., Duan, N., Wu, S., Dai, R., Wang, Z., and Li, X. (2016). Impedimetric *Salmonella* aptasensor using a glassy carbon electrode modified with an electrodeposited composite consisting of reduced graphene oxide and carbon nanotubes. *Microchimica Acta* 183, 337–344. doi: 10.1007/s00604-015-1649-7

Jia, W., Li, H., Wilkop, T., Liu, X., Yu, X., Cheng, Q., et al. (2018). Silver decahedral nanoparticles empowered SPR imaging-SELEX for high throughput screening of aptamers with real-time assessment. *Biosensors Bioelectronics* 109, 206–213. doi: 10.1016/j.bios.2018.02.029

Jia, F., Xu, L., Yan, W., Wu, W., Yu, Q., Tian, X., et al. (2017). A magnetic relaxation switch aptasensor for the rapid detection of Pseudomonas aeruginosa using superparamagnetic nanoparticles. *Microchimica Acta* 184, 1539–1545. doi: 10.1007/s00604-017-2142-2

Jiang, L., Wang, H., and Chen, S. (2020). Aptamer (AS1411)-conjugated liposome for enhanced therapeutic efficacy of mirna-29b in ovarian cancer. *J. Nanoscience Nanotechnology* 20, 2025–2031. doi: 10.1166/jnn.2020.17301

Johnson, J. R. (1991). Virulence factors in *Escherichia coli* urinary tract infection. *Clin. Microbiol. Rev.* 4, 80–128. doi: 10.1128/CMR.4.1.80

Jonsson, S., Musher, D. M., Chapman, A., Goree, A., and Lawrence, E. C. (1985). Phagocytosis and killing of common bacterial pathogens of the lung by human alveolar macrophages. *J. Infect. Dis.* 152, 4–13. doi: 10.1093/infdis/152.1.4

Kadurugamuwa, J. L., and Beveridge, T. J. (1995). Virulence factors are released from pseudomonas aeruginosa in association with membrane vesicles during normal growth and exposure to gentamicin: a novel mechanism of enzyme secretion. *J. Bacteriol.* 177 (14), 3998–4008. doi: 10.1128/jb.177.14.3998-4008.1995

Kalra, P., Mishra, S. K., Kaur, S., Kumar, A., Prasad, H. K., Sharma, T. K., et al. (2018). G-Quadruplex-forming DNA aptamers inhibit the dna-binding function of HupB and *Mycobacterium tuberculosis* entry into host cells. *Mol. Ther. Nucleic Acids* 13, 99–109. doi: 10.1016/j.omtn.2018.08.011

Kamiyama, N., Soma, R., Hidano, S., Watanabe, K., Umekita, H., Fukuda, C., et al. (2017). Ribavirin inhibits Zika virus (ZIKV) replication in *vitro* and suppresses viremia in ZIKV-infected STAT1-deficient mice. *Antiviral Res.* 146, 1–11. doi: 10.1016/j.antiviral.2017.08.007

Kaper, J. B., Nataro, J. P., and Mobley, H. L. T. (2004). Pathogenic *escherichia coli*. *Nat. Rev. Microbiol.* 2, 123–140. doi: 10.1038/nrmicro818

Kaur, H., Shorie, M., and Sabherwal, P. (2020). Electrochemical aptasensor using boron-carbon nanorods decorated by nickel nanoparticles for detection of E. coli O157: H7. *Microchimica Acta* 187, 461. doi: 10.1007/s00604-020-04444-y

Kaur, H., Shorie, M., Sharma, M., Ganguli, A. K., and Sabherwal, P. (2017). Bridged rebar graphene functionalized aptasensor for pathogenic E. coli O78:K80:H11 detection. *Biosensors Bioelectronics* 98, 486–493. doi: 10.1016/j.bios.2017.07.004

Keefe, A. D., Pai, S., and Ellington, A. (2010). Aptamers as therapeutics. *Nat. Rev. Drug Discovery* 9, 537–550. doi: 10.1038/nrd3141

Keller, L. E., Jones, C. V., Thornton, J. A., Sanders, M. E., Swiatlo, E., Nahm, M. H., et al. (2013). PspK of *Streptococcus pneumoniae* increases adherence to epithelial cells and enhances nasopharyngeal colonization. *Infection Immun.* 81, 173–181. doi: 10.1128/IAI.00755-12

Ker, D. S., Jenkins, H. T., Greive, S. J., and Antson, A. A. (2021). CryoEM structure of the Nipah virus nucleocapsid assembly. *PLoS Pathog.* 17 (7), e1009740. doi: 10.1371/journal.ppat.1009740

Kim, B., Chung, K. W., and Lee, J. H. (2018a). Non-stop aptasensor capable of rapidly monitoring norovirus in a sample. *J. Pharm. Biomed. Anal.* 152, 315–321. doi: 10.1016/j.jpba.2018.02.022

Kim, S., Lee, S., and Lee, H. J. (2018b). An aptamer-aptamer sandwich assay with nanorod-enhanced surface plasmon resonance for attomolar concentration of norovirus capsid protein. *Sensors Actuators B: Chem.* 273, 1029–1036. doi: 10.1016/j.snb.2018.06.108

Kim, E. S., Lu, C., Khuri, F. R., Tonda, M., Glisson, B. S., Liu, D., et al. (2001). A phase II study of STEALTH cisplatin (SPI-77) in patients with advanced non-small cell lung cancer. *Lung Cancer* 34, 427–432. doi: 10.1016/S0169-5002(01)00278-1

Kinghorn, A., Fraser, L., Liang, S., Shiu, S., and Tanner, J. (2017). Aptamer bioinformatics. *Int. J. Mol. Sci.* 18, 2516. doi: 10.3390/ijms18122516

Komarova, N., and Kuznetsov, A. (2019). Inside the black box: what makes SELEX better? *Molecules* 24, 3598. doi: 10.3390/molecules24193598

Kong, H. Y., and Byun, J. (2013). Nucleic acid aptamers: new methods for selection, stabilization, and application in biomedical science. *Biomolecules Ther.* 21, 423–434. doi: 10.4062/biomolther.2013.085

Kovacevic, K. D., Gilbert, J. C., and Jilma, B. (2018). Pharmacokinetics, pharmacodynamics and safety of aptamers. *Advanced Drug Delivery Rev.* 134, 36–50. doi: 10.1016/j.addr.2018.10.008

Kristian, S. A., Hwang, J. H., Hall, B., Leire, E., Iacomini, J., Old, R., et al. (2015). Retargeting pre-existing human antibodies to a bacterial pathogen with an alpha-Gal conjugated aptamer. *J. Mol. Med.* 93, 619–631. doi: 10.1007/s00109-015-1280-4

Krüger, A., de Jesus Santos, A. P., de Sá, V., Ulrich, H., and Wrenger, C. (2021). Aptamer applications in emerging viral diseases. *Pharmaceuticals* 14, 622. doi: 10.3390/ph14070622

Ku, T.-H., Zhang, T., Luo, H., Yen, T., Chen, P.-W., Han, Y., et al. (2015). Nucleic acid aptamers: an emerging tool for biotechnology and biomedical sensing. *Sensors* 15, 16281–16313. doi: 10.3390/s150716281

Kumar De, S., Ray, S., Rawat, Y., Mondal, S., Nandy, A., Verma, P., et al. (2021). Porous Au-seeded Ag nanorod networks conjugated with DNA aptamers for impedimetric sensing of DENV-2. *Sensors Actuators B: Chem.* 348, 130709. doi: 10.1016/j.snb.2021.130709

Kusumawati, A., Mustopa, A. Z., Umami, R. N., Santoso, A., Wibawan, I. W. T., Setiyono, A., et al. (2022). Antibiofilm activity and binding specificity of polyclonal dna aptamers on *Staphylococcus aureus* and *Escherichia coli*. *Microbiol. Biotechnol. Lett.* 50, 328–336. doi: 10.48022/mbl.2206.06001

Kwong Hong Tsang, D., Lieberthal, T. J., Watts, C., Dunlop, I. E., Ramadan, S., del Rio Hernandez, A. E., et al. (2019). Chemically functionalised graphene fet biosensor for the label-free sensing of exosomes. *Sci. Rep.* 9, 13946. doi: 10.1038/s41598-019-50412-9

Lai, H.-C., Wang, C.-H., Liou, T.-M., and Lee, G.-B. (2014). Influenza A virus-specific aptamers screened by using an integrated microfluidic system. *Lab. Chip* 14, 2002–2013. doi: 10.1039/C4LC00187G

Lebars, I., Richard, T., Di Primo, C., and Toulmé, J.-J. (2007). LNA derivatives of a kissing aptamer targeted to the trans-activating responsive RNA element of HIV-1. *Blood Cells Molecules Dis.* 38, 204–209. doi: 10.1016/j.bcmd.2006.11.008

Ledlod, S., Areekit, S., Santiwatanakul, S., and Chansiri, K. (2020). Colorimetric aptasensor for detecting Salmonella spp., *Listeria monocytogenes*, and *Escherichia coli* in meat samples. *Food Sci. Technol. Int.* 26, 430–443. doi: 10.1177/1082013219899593

Lee, C. H., Lee, S.-H., Kim, J. H., Noh, Y.-H., Noh, G.-J., and Lee, S.-W. (2015). Pharmacokinetics of a cholesterol-conjugated aptamer against the Hepatitis C Virus (HCV) NS5B protein. *Mol. Ther. - Nucleic Acids* 4, e254. doi: 10.1038/mtna.2015.30

Lee, J. Y., Nguyen, T. T. N., and Myoung, J. (2020). Zika virus-encoded NS2A and NS4A strongly downregulate NF-κB promoter activity. *J. Microbiol. Biotechnol.* 30, 1651–1658. doi: 10.4014/JMB.2011.11003

Lee, B., Park, J., Ryu, M., Kim, S., Joo, M., Yeom, J. H., et al. (2017). Antimicrobial peptide-loaded gold nanoparticle-DNA aptamer conjugates as highly effective antibacterial therapeutics against Vibrio vulnificus. *Sci. Rep.* 7 (1), 13572. doi: 10.1038/s41598-017-14127-z

Lerminiaux, N. A., MacKenzie, K. D., and Cameron, A. D. S. (2020). *Salmonella* pathogenicity island 1 (spi-1): the evolution and stabilization of a core genomic type three secretion system. *Microorganisms* 8, 576. doi: 10.3390/microorganisms8040576

Leung, D. W., Prins, K. C., Basler, C. F., and Amarasinghe, G. K. (2010). Ebolavirus VP35 is a multifunctional virulence factor. *Virulence* 1, 526–531. doi: 10.4161/viru.1.6.12984

Li, Y., Chen, M., Fan, X., Peng, J., Pan, L., Tu, K., et al. (2022). Sandwich fluorometric method for dual-role recognition of *Listeria monocytogenes* based on antibiotic-affinity strategy and fluorescence quenching effect. *Analytica Chimica Acta* 1221, 340085. doi: 10.1016/j.aca.2022.340085

Li, T., Ou, G., Chen, X., Li, Z., Hu, R., Li, Y., et al. (2020). Naked-eye based point-of-care detection of *E.coli* O157: H7 by a signal-amplified microfluidic aptasensor. *Analytica Chimica Acta* 1130, 20–28. doi: 10.1016/j.aca.2020.07.031

Li, J., Yun, W., Zhang, H., Chen, L., Ho, H.-P., Pu, X., et al. (2023). MoS2 nanosheets based label-free colorimetric aptasensor for *Escherichia coli* O157: H7 detection. *Colloids Surfaces A: Physicochemical Eng. Aspects* 674, 131955. doi: 10.1016/j.colsurfa.2023.131955

Li, A., Zuo, P., and Ye, B.-C. (2021). An aptamer biosensor based dual signal amplification system for the detection of Salmonella typhimurium. *Analytical Biochem.* 615, 114050. doi: 10.1016/j.ab.2020.114050

Lier, C., Becker, S., and Biedenkopf, N. (2017). Dynamic phosphorylation of Ebola virus VP30 in NP-induced inclusion bodies. *Virology* 512, 39–47. doi: 10.1016/j.virol.2017.09.006

Lijuan, C., Xing, Y., Minxi, W., Wenkai, L., and Le, D. (2017). Development of an aptamer-ampicillin conjugate for treating biofilms. *Biochem. Biophys. Res. Commun.* 483, 847–854. doi: 10.1016/j.bbrc.2017.01.016

Liu, R., Zhang, Y., Ali, S., Haruna, S. A., He, P., Li, H., et al. (2021). Development of a fluorescence aptasensor for rapid and sensitive detection of Listeria monocytogenes in food. *Food Control* 122, 107808. doi: 10.1016/j.foodcont.2020.107808

Lum, J., Wang, R., Hargis, B., Tung, S., Bottje, W., Lu, H., et al. (2015). An impedance aptasensor with microfluidic chips for specific detection of H5N1 avian influenza virus. *Sensors* 15, 18565–18578. doi: 10.3390/s150818565

Lunardelli, V. A. S., Almeida, B. S., Apostolico, J. S., Rezende, T., Yamamoto, M. M., Pereira, S. S., et al. (2023). Diagnostic and vaccine potential of Zika virus envelope protein (E) derivates produced in bacterial and insect cells. *Front. Immunol.* 14. doi: 10.3389/fimmu.2023.1071041

Ma, X., Xie, L., Wartchow, C., Warne, R., Xu, Y., Rivkin, A., et al. (2017). Structural basis for therapeutic inhibition of influenza A polymerase PB2 subunit. *Sci. Rep.* 7 (1), 9385. doi: 10.1038/s41598-017-09538-x

Ma, X., Xu, X., Xia, Y., and Wang, Z. (2018). SERS aptasensor for *Salmonella typhimurium* detection based on spiny gold nanoparticles. *Food Control* 84, 232–237. doi: 10.1016/j.foodcont.2017.07.016

Maasch, C., Buchner, K., Eulberg, D., Vonhoff, S., and Klussmann, S. (2008). Physicochemical stability of NOX-E36, a 40mer L-RNA (Spiegelmer) for therapeutic applications. *Nucleic Acids Symposium Ser.* 52, 61–62. doi: 10.1093/nass/nrn031

Majdinasab, M., Badea, M., and Marty, J. L. (2022). Aptamer-based lateral flow assays: current trends in clinical diagnostic rapid tests. *Pharmaceuticals* 15, 90. doi: 10.3390/ph15010090

Marton, S., Cleto, F., Krieger, M. A., and Cardoso, J. (2016). Isolation of an aptamer that binds specifically to E. coli. *PLoS One* 11, e0153637. doi: 10.1371/journal.pone.0153637

Matchawong, A., Srisawat, C., Sangboonruang, S., and Tharinjaroen, C. S. (2022). The ability of nuclease-resistant RNA aptamer against *Streptococcus suis* Serotype 2, Strain P1/7 to reduce biofilm formation in *vitro*. *Molecules* 27, 3894. doi: 10.3390/molecules27123894

Mayer, G., Ahmed, M.-S. L., Dolf, A., Endl, E., Knolle, P. A., and Famulok, M. (2010). Fluorescence-activated cell sorting for aptamer SELEX with cell mixtures. *Nat. Protoc.* 5, 1993–2004. doi: 10.1038/nprot.2010.163

McAuley, J. L., Gilbertson, B. P., Trifkovic, S., Brown, L. E., and McKimm-Breschkin, J. L. (2019). Influenza virus neuraminidase structure and functions. *Front. Microbiol.* 10. doi: 10.3389/fmicb.2019.00039

Mishra, A., Pilloton, R., Jain, S., Roy, S., Khanuja, M., Mathur, A., et al. (2022). Paper-based electrodes conjugated with tungsten disulfide nanostructure and aptamer for impedimetric detection of *Listeria monocytogenes*. *Biosensors* 12, 88. doi: 10.3390/bios12020088

Mok, J., Jeon, J., Jo, J., Kim, E., and Ban, C. (2021). Novel one-shot fluorescent aptasensor for dengue fever diagnosis using NS1-induced structural change of G-quadruplex aptamer. *Sensors Actuators B: Chem.* 343, 130077. doi: 10.1016/j.snb.2021.130077

Moon, J., Kim, G., Lee, S., and Park, S. (2013). Identification of *Salmonella Typhimurium*-specific DNA aptamers developed using whole-cell SELEX and FACS analysis. *J. Microbiological Methods* 95, 162–166. doi: 10.1016/j.mimet.2013.08.005

Mori, Y., Nakamura, Y., and Ohuchi, S. (2012). Inhibitory RNA aptamer against SP6 RNA polymerase. *Biochem. Biophys. Res. Commun.* 420, 440–443. doi: 10.1016/j.bbrc.2012.03.014

Muniandy, S., Teh, S. J., Appaturi, J. N., Thong, K. L., Lai, C. W., Ibrahim, F., et al. (2019). A reduced graphene oxide-titanium dioxide nanocomposite based electrochemical aptasensor for rapid and sensitive detection of Salmonella enterica. *Bioelectrochemistry* 127, 136–144. doi: 10.1016/j.bioelechem.2019.02.005

Musafia, B., Oren-Banaroya, R., and Noiman, S. (2014). Designing anti-influenza aptamers: Novel quantitative structure activity relationship approach gives insights into aptamer – virus interaction. *PLoS One* 9, e97696. doi: 10.1371/journal.pone.0097696

Nguyen, V.-T., Kwon, Y. S., Kim, J. H., and Gu, M. B. (2014). Multiple GO-SELEX for efficient screening of flexible aptamers. *Chem. Commun.* 50, 10513–10516. doi: 10.1039/C4CC03953J

Ni, S., Yao, H., Wang, L., Lu, J., Jiang, F., Lu, A., et al. (2017). Chemical modifications of nucleic acid aptamers for therapeutic purposes. *Int. J. Mol. Sci.* 18, 1683. doi: 10.3390/ijms18081683

Ni, S., Zhuo, Z., Pan, Y., Yu, Y., Li, F., Liu, J., et al. (2021). Recent progress in aptamer discoveries and modifications for therapeutic applications. *ACS Appl. Materials Interfaces* 13, 9500–9519. doi: 10.1021/acsami.0c05750

Ning, Y., Wang, X., Chen, P., Liu, S., Hu, J., Xiao, R., et al. (2022). Targeted inhibition of methicillin-resistant Staphylococcus aureus biofilm formation by a graphene oxide-loaded aptamer/berberine bifunctional complex. *Drug Delivery* 29, 1675–1683. doi: 10.1080/10717544.2022.2079768

Ninomiya, K., Yamashita, T., Kawabata, S., and Shimizu, N. (2014). Targeted and ultrasound-triggered drug delivery using liposomes co-modified with cancer cell-targeting aptamers and a thermosensitive polymer. *Ultrasonics Sonochemistry* 21, 1482–1488. doi: 10.1016/j.ultsonch.2013.12.023

Nishimoto, K. P., Newkirk, D., Hou, S., Fruehauf, J., and Nelson, E. L. (2007). Fluorescence activated cell sorting (FACS) using RNAlater to minimize RNA degradation and perturbation of mRNA expression from cells involved in initial host microbe interactions. *J. Microbiological Methods* 70, 205–208. doi: 10.1016/j.mimet.2007.03.022

Nishimoto, A. T., Rosch, J. W., and Tuomanen, E. I. (2020). Pneumolysin: pathogenesis and therapeutic target. *Front. Microbiol.* 11. doi: 10.3389/fmicb.2020.01543

Nobusawa, E. (1997). Structure and function of the hemagglutinin of influenza viruses. *Nihon Rinsho* 55, 2562–2569. Japanese Journal of Clinical Medicine.

Nutho, B., Mulholland, A. J., and Rungrotmongkol, T. (2019). The reaction mechanism of Zika virus NS2B/NS3 serine protease inhibition by dipeptidyl

aldehyde: A QM/MM study. *Phys. Chem. Chem. Phys.* 21, 14945–14956. doi: 10.1039/c9cp02377a

O'Neill, R. E., Talon, J., and Palese, P. (1998). The influenza virus NEP (NS2 protein) mediates the nuclear export of viral ribonucleoproteins. *EMBO J.* 17 (1), 288–296. doi: 10.1093/emboj/17.1.288

Ohuchi, S. (2012). Cell-SELEX technology. *Biores. Open Access* 1, 265–272. doi: 10.1089/biores.2012.0253

Ommen, P., Hansen, L., Hansen, B. K., Vu-Quang, H., Kjems, J., and Meyer, R. L. (2022). Aptamer-targeted drug delivery for *Staphylococcus aureus* biofilm. *Front. Cell. Infection Microbiol.* 12. doi: 10.3389/fcimb.2022.814340

Oravczová, V., Tatarko, M., Süle, J., Hun, M., Kerényi, Z., Hucker, A., et al. (2020). Detection of Listeria innocua by acoustic aptasensor. In *Proceedings*. MDPI 60 (1), 8. doi: 10.3390/IECB2020-07079

Oroh, S. B., Mustopa, A. Z., Budiarti, S., and Budiarto, B. R. (2020). Inhibition of enteropathogenic *Escherichia coli* biofilm formation by DNA aptamer. *Mol. Biol. Rep.* 47, 7567–7573. doi: 10.1007/s11033-020-05822-8

Otte, D.-M., Choukeife, M., Patwari, T., and Mayer, G. (2022). "Nucleic acid aptamers: from basic research to clinical applications," in *Handbook of chemical Biology of Nucleic Acids* (Springer Nature, Singapore), 1–25. doi: 10.1007/978-981-16-1313-5_25-1

Otto, M. (2014). *Staphylococcus aureus* toxins. *Curr. Opin. In Microbiol.* 17, 32–37. doi: 10.1016/j.mib.2013.11.004

Palacio, I., Moreno, M., Náñez, A., Purwidyantri, A., Domingues, T., Cabral, P. D., et al. (2023). Attomolar detection of hepatitis C virus core protein powered by molecular antenna-like effect in a graphene field-effect aptasensor. *Biosensors Bioelectronics* 222, 115006. doi: 10.1016/j.bios.2022.115006

Palmqvist, N., Foster, T., Tarkowski, A., and Josefsson, E. (2002). Protein A is a virulence factor in *Staphylococcus aureus* arthritis and septic death. *Microbial Pathogenesis* 33, 239–249. doi: 10.1006/mpat.2002.0533

Pan, Q., Zhang, X. L., Wu, H. Y., He, P. W., Wang, F., Zhang, M. S., et al. (2005). Aptamers that preferentially bind type IVB pili and inhibit human monocytic-cell invasion by *Salmonella enterica* serovar typhi. *Antimicrobial Agents Chemotherapy* 49, 4052–4060. doi: 10.1128/AAC.49.10.4052-4060.2005

Pang, Y., Rong, Z., Wang, J., Xiao, R., and Wang, S. (2015). A fluorescent aptasensor for H5N1 influenza virus detection based-on the core–shell nanoparticles metal-enhanced fluorescence (MEF). *Biosensors Bioelectronics* 66, 527–532. doi: 10.1016/j.bios.2014.10.052

Park, G., Lee, M., Kang, J., Park, C., Min, J., and Lee, T. (2022). Selection of DNA aptamer and its application as an electrical biosensor for Zika virus detection in human serum. *Nano Convergence* 9, 41. doi: 10.1186/s40580-022-00332-8

Park, H., Lee, H., Lee, M., Baek, C., Park, J. A., Jang, M., et al. (2023). Synthesis of isolated DNA aptamer and its application of AC-electrothermal flow-based rapid biosensor for the detection of dengue virus in a spiked sample. *Bioconjugate Chem.* 34, 1486–1497. doi: 10.1021/acs.bioconjchem.3c00249

Pathania, P., Sharma, A., Kumar, B., Rishi, P., and Raman Suri, C. (2017). Selective identification of specific aptamers for the detection of non-typhoidal salmonellosis in an apta-impedimetric sensing format. *Microchimica Acta* 184, 1499–1508. doi: 10.1007/s00604-017-2098-2

Pebdeni, A. B., Hosseini, M., and Ganjali, M. R. (2020). Fluorescent turn-on aptasensor of *Staphylococcus aureus* based on the FRET between green carbon quantum dot and gold nanoparticle. *Food Analytical Methods* 13, 2070–2079. doi: 10.1007/s12161-020-01821-4

Perschbacher, K., Smestad, J. A., Peters, J. P., Standiford, M. M., Denic, A., Wootla, B., et al. (2015). Quantitative PCR Analysis of DNA aptamer pharmacokinetics in mice. *Nucleic Acid Ther.* 25, 11–19. doi: 10.1089/nat.2014.0515

Petrišič, N., Kozorog, M., Aden, S., Podobnik, M., and Anderluh, G. (2021). The molecular mechanisms of listeriolysin O-induced lipid membrane damage. *Biochim. Biophys. Acta (BBA) - Biomembranes* 1863, 183604. doi: 10.1016/j.bbamem.2021.183604

Pfander, S., Fiammengo, R., Kirin, S. I., Metzler-Nolte, N., and Jäschke, A. (2007). Reversible site-specific tagging of enzymatically synthesized RNAs with aldehyde–hydrazine chemistry and protease-cleavable linkers. *Nucleic Acids Res.* 35, e25. doi: 10.1093/nar/gkl1110

Pistor, S., Chakraborty, T., Niebuhr, K., Domann, E., and Wehland, J. (1994). The ActA protein of *Listeria monocytogenes* acts as a nucleator inducing reorganization of the actin cytoskeleton. *EMBO J.* 13, 758–763. doi: 10.1002/j.1460-2075.1994.tb06318.x

Portnoy, D. A., Jacks, P. S., and Hinrichs, D. J. (1988). Role of hemolysin for the intracellular growth of Listeria monocytogenes. *J Exp Med.* 167 (4), 1459–1471. doi: 10.1084/jem.167.4.1459

Qi, X., Ye, Y., Wang, H., Zhao, B., Xu, L., Zhang, Y., et al. (2022). An ultrasensitive and dual-recognition SERS biosensor based on Fe3O4@Au-Teicoplanin and aptamer functionalized Au@Ag nanoparticles for detection of *Staphylococcus aureus*. *Talanta* 250, 123648. doi: 10.1016/j.talanta.2022.123648

Raddatz, M. L., Dolf, A., Endl, E., Knolle, P., Famulok, M., and Mayer, G. (2008). Enrichment of cell-targeting and population-specific aptamers by fluorescence-activated cell sorting. *Angewandte Chemie Int. Edition* 47, 5190–5193. doi: 10.1002/anie.200800216

Raffatellu, M., Wilson, R. P., Chessa, D., Andrews-Polymenis, H., Tran, Q. T., Lawhon, S., et al. (2005). SipA, SopA, SopB, SopD, and SopE2 Contribute to *Salmonella enterica* serotype typhimurium invasion of epithelial cells. *Infection Immun.* 73, 146–154. doi: 10.1128/IAI.73.1.146-154.2005

Rahbi, F. A., Salmi, I. A., Khamis, F., Balushi, Z. A., Pandak, N., Petersen, E., et al. (2023). Physicians' attitudes, knowledge, and practices regarding antibiotic prescriptions. *J. Global Antimicrobial Resistance* 32, 58–65. doi: 10.1016/j.jgar.2022.12.005

Raji, M. A., Suaifan, G., Shibl, A., Weber, K., Cialla-May, D., Popp, J., et al. (2021). Aptasensor for the detection of Methicillin resistant *Staphylococcus aureus* on contaminated surfaces. *Biosensors Bioelectronics* 176, 112910. doi: 10.1016/j.bios.2020.112910

Ramanathan, S., Gopinath, S. C. B., Ismail, Z. H., Md Arshad, M. K., and Poopalan, P. (2022). Aptasensing nucleocapsid protein on nanodiamond assembled gold interdigitated electrodes for impedimetric SARS-CoV-2 infectious disease assessment. *Biosensors Bioelectronics* 197, 113735. doi: 10.1016/j.bios.2021.113735

Ranadheera, C., Proulx, R., Chaiyakul, M., Jones, S., Grolla, A., Leung, A., et al. (2018). The interaction between the Nipah virus nucleocapsid protein and phosphoprotein regulates virus replication. *Sci. Rep.* 8 (1), 15994. doi: 10.1038/s41598-018-34484-7

Ranjbar, S., and Shahrokhian, S. (2018). Design and fabrication of an electrochemical aptasensor using Au nanoparticles/carbon nanoparticles/cellulose nanofibers nanocomposite for rapid and sensitive detection of Staphylococcus aureus. *Bioelectrochemistry* 123, 70–76. doi: 10.1016/j.bioelechem.2018.04.018

Rastogi, M., and Singh, S. K. (2020). Zika virus NS1 affects the junctional integrity of human brain microvascular endothelial cells. *Biochimie* 176, 52–61. doi: 10.1016/j.biochi.2020.06.011

Reich, P., Stoltenburg, R., Strehlitz, B., Frense, D., and Beckmann, D. (2017). Development of an impedimetric aptasensor for the detection of *Staphylococcus aureus*. *Int. J. Mol. Sci.* 18, 2484. doi: 10.3390/ijms18112484

Ren, J., Liang, G., Man, Y., Li, A., Jin, X., Liu, Q., et al. (2019). Aptamer-based fluorometric determination of *Salmonella typhimurium* using Fe3O4 magnetic separation and CdTe quantum dots. *PLoS One* 14, e0218325. doi: 10.1371/journal.pone.0218325

Reverdatto, S., Burz, D., and Shekhtman, A. (2015). Peptide aptamers: Development and applications. *Curr. Topics Medicinal Chem.* 15, 1082–1101. doi: 10.2174/1568026615666150413153143

RM, R., Maroli, N., J, A., Ponmalai, K., and K, K. (2020). Highly adaptable and sensitive FRET-based aptamer assay for the detection of Salmonella paratyphi A. *Spectrochimica Acta Part A: Mol. Biomolecular Spectrosc.* 243, 118662. doi: 10.1016/j.saa.2020.118662

Roberts, P. C., Lamb, R. A., and Compans, R. W. (1998). The M1 and M2 proteins of influenza A virus are important determinants in filamentous particle formation. *Virology* 240 (1), 127–137. doi: 10.1006/viro.1997.8916

Roushani, M., Sarabaegi, M., and Pourahmad, F. (2019). Impedimetric aptasensor for Pseudomonas aeruginosa by using a glassy carbon electrode modified with silver nanoparticles. *Microchimica Acta* 186, 725. doi: 10.1007/s00604-019-3858-y

Roxo, C., Kotkowiak, W., and Pasternak, A. (2019). G-Quadruplex-forming aptamers—characteristics, applications, and perspectives. *Molecules* 24, 3781. doi: 10.3390/molecules24203781

Sanjuán, R. (2012). From molecular genetics to phylodynamics: evolutionary relevance of mutation rates across viruses. *PLoS Pathog.* 8, e1002685. doi: 10.1371/journal.ppat.1002685

Saravanan, H., Subramani, T., Rajaramon, S., David, H., Sajeevan, A., Sujith, S., et al. (2023). Exploring nanocomposites for controlling infectious microorganisms: charting the path forward in antimicrobial strategies. *Front. Pharmacol.* 14. doi: 10.3389/fphar.2023.1282073

Schasfoort, R. B. M. (2017). "Introduction to surface plasmon resonance," in *handbook of surface plasmon resonance* (The Royal Society of Chemistry), 1–26. doi: 10.1039/9781788010283-00001

Schmitz, F. R. W., Cesca, K., Valério, A., de Oliveira, D., and Hotza, D. (2023). Colorimetric detection of *Pseudomonas aeruginosa* by aptamer-functionalized gold nanoparticles. *Appl. Microbiol. Biotechnol.* 107, 71–80. doi: 10.1007/s00253-022-12283-5

Shang, Z., Song, H., Shi, Y., Qi, J., and Gao, G. F. (2018). Crystal structure of the capsid protein from zika virus. *J. Mol. Biol.* 430, 948–962. doi: 10.1016/j.jmb.2018.02.006

Shatila, F., Yalçın, H. T., Özyurt, C., Evran, S., Çakır, B., Yaşa, İ., et al. (2020a). Single-stranded DNA (ssDNA) Aptamer targeting SipA protein inhibits Salmonella Enteritidis invasion of intestinal epithelial cells. *Int. J. Biol. Macromolecules* 148, 518–524. doi: 10.1016/j.ijbiomac.2020.01.132

Shatila, F., Yaşa, İ., and Yalçın, H. T. (2020b). Inhibition of Salmonella enteritidis biofilms by *Salmonella* invasion protein-targeting aptamer. *Biotechnol. Lett.* 42, 1963–1974. doi: 10.1007/s10529-020-02920-2

Shaw, M. L., Garciía-Sastre, A., Palese, P., and Basler, C. F. (2004). Nipah Virus V and W proteins have a common stat1-binding domain yet inhibit STAT1 activation from the cytoplasmic and nuclear compartments, respectively. *J. Virol.* 78, 5633–5641. doi: 10.1128/JVI.78.11.5633-5641.2004

Shraim, A. S., Abdel Majeed, B. A., Al-Binni, M. A., and Hunaiti, A. (2022). Therapeutic potential of aptamer–protein interactions. *ACS Pharmacol. Trans. Sci.* 5, 1211–1227. doi: 10.1021/acsptsci.2c00156

Siddiqui, M. A. A., and Keating, G. M. (2005). Pegaptanib. *Drugs* 65, 1571–1577. doi: 10.2165/00003495-200565110-00010

Singh, N. K., Ray, P., Carlin, A. F., Magallanes, C., Morgan, S. C., Laurent, L. C., et al. (2021). Hitting the diagnostic sweet spot: Point-of-care SARS-CoV-2 salivary antigen testing with an off-the-shelf glucometer. *Biosensors Bioelectronics* 180, 113111. doi: 10.1016/j.bios.2021.113111

Sohouli, E., Ghalkhani, M., Zargar, T., Joseph, Y., Rahimi-Nasrabadi, M., Ahmadi, F., et al. (2022). A new electrochemical aptasensor based on gold/nitrogen-doped carbon nano-onions for the detection of *Staphylococcus aureus*. *Electrochimica Acta* 403, 139633. doi: 10.1016/j.electacta.2021.139633

Sola, M., Menon, A. P., Moreno, B., Meraviglia-Crivelli, D., Soldevilla, M. M., Cartón-García, F., et al. (2020). Aptamers against live targets: is *in vivo* SELEX finally coming to the edge? *Mol. Ther. - Nucleic Acids* 21, 192–204. doi: 10.1016/j.omtn.2020.05.025

Somerville, J. E. Jr., Cassiano, L., and Darveau, R. P. (1999). *Escherichia coli* msbB Gene as a virulence factor and a therapeutic target. *Infection Immun.* 67 (12), 6583–6590. doi: 10.1128/IAI.67.12.6583-6590.1999

Sreejit, G., Ahmed, A., Parveen, N., Jha, V., Valluri, V. L., Ghosh, S., et al. (2014). The ESAT-6 Protein of *Mycobacterium tuberculosis* interacts with Beta-2-Microglobulin (β2M) affecting antigen presentation function of macrophage. *PLoS Pathog.* 10, e1004446. doi: 10.1371/journal.ppat.1004446

Srivastava, S., Abraham, P. R., and Mukhopadhyay, S. (2021). Aptamers: An emerging tool for diagnosis and therapeutics in tuberculosis. *Front. Cell. Infection Microbiol.* 11. doi: 10.3389/fcimb.2021.656421

Sudagidan, M., Yildiz, G., Onen, S., Al, R., Temiz, Ş.N., Yurt, M. N. Z., et al. (2021). Targeted mesoporous silica nanoparticles for improved inhibition of disinfectant resistant *Listeria monocytogenes* and lower environmental pollution. *J. Hazardous Materials* 418, 126364. doi: 10.1016/j.jhazmat.2021.126364

Suenaga, E., and Kumar, P. K. R. (2014). An aptamer that binds efficiently to the hemagglutinins of highly pathogenic avian influenza viruses (H5N1 and H7N7) and inhibits hemagglutinin–glycan interactions. *Acta Biomaterialia* 10, 1314–1323. doi: 10.1016/j.actbio.2013.12.034

Sun, B., Jia, L., Liang, B., Chen, Q., and Liu, D. (2018). Phylogeography, transmission, and viral proteins of Nipah Virus. *Virologica Sin.* 33, 385–393. doi: 10.1007/s12250-018-0050-1

Sun, J., Siroy, A., Lokareddy, R. K., Speer, A., Doornbos, K. S., Cingolani, G., et al. (2015). The tuberculosis necrotizing toxin kills macrophages by hydrolyzing NAD. *Nat. Struct. Mol. Biol.* 22, 672–678. doi: 10.1038/nsmb.3064

Sun, H., Zhu, X., Lu, P. Y., Rosato, R. R., Tan, W., and Zu, Y. (2014). Oligonucleotide aptamers: New tools for targeted cancer therapy. *Mol. Ther. - Nucleic Acids* 3, e182. doi: 10.1038/mtna.2014.32

Terlizzi, M. E., Gribaudo, G., and Maffei, M. E. (2017). UroPathogenic *Escherichia coli* (UPEC) infections: Virulence factors, bladder responses, antibiotic, and non-antibiotic antimicrobial strategies. *Front. Microbiol.* 8. doi: 10.3389/fmicb.2017.01566

Thevendran, R., Rogini, S., Leighton, G., Mutombwera, A., Shigdar, S., Tang, T.-H., et al. (2023). The diagnostic potential of RNA aptamers against the NS1 protein of dengue virus serotype 2. *Biology* 12, 722. doi: 10.3390/biology12050722

Thiviyanathan, V., Somasunderam, A. D., and Gorenstein, D. G. (2007). Combinatorial selection and delivery of thioaptamers. *Biochem. Soc. Trans.* 35, 50–52. doi: 10.1042/BST0350050

Tran, Q. T., Gomez, G., Khare, S., Lawhon, S. D., Raffatellu, M., Baöumler, A. J., et al. (2010). The *Salmonella enterica* Serotype typhi Vi capsular antigen is expressed after the bacterium enters the ileal mucosa. *Infection Immun.* 78, 527–535. doi: 10.1128/IAI.00972-09

Turgis, M., Khanh, D. V., Majid, J., Behnoush, M., and Monique, L. (2016). Synergistic antimicrobial effect of combined bacteriocins against food pathogens and spoilage bacteria. *Microb. Res. Inter.* 4 (1), 1–5.

Turner, J., and Torrelles, J. B. (2018). Mannose-capped lipoarabinomannan in Mycobacterium tuberculosis pathogenesis. *Pathog Dis.* 76 (4), fty026. doi: 10.1093/femspd/fty026

Turrell, L., Lyall, J. W., Tiley, L. S., Fodor, E., and Vreede, F. T. (2013). The role and assembly mechanism of nucleoprotein in influenza A virus ribonucleoprotein complexes. *Nat. Commun.* 4 (1), 1591. doi: 10.1038/ncomms2589

Ucak, S., Sudagidan, M., Borsa, B. A., Mansuroglu, B., and Ozalp, V. C. (2020). Inhibitory effects of aptamer targeted teicoplanin encapsulated PLGA nanoparticles for *Staphylococcus aureus* strains. *World J. Microbiol. Biotechnol.* 36 (5), 69. doi: 10.1007/s11274-020-02845-y

Uemachi, H., Kasahara, Y., Tanaka, K., Okuda, T., Yoneda, Y., and Obika, S. (2021). Hybrid-Type SELEX for the selection of artificial nucleic acid aptamers exhibiting cell internalization activity. *Pharmaceutics* 13, 888. doi: 10.3390/pharmaceutics13060888

Uniyal, A., Srivastava, G., Pal, A., Taya, S., and Muduli, A. (2023). Recent advances in optical biosensors for sensing applications: a review. *Plasmonics* 18, 735–750. doi: 10.1007/s11468-023-01803-2

Valente, A. P., and Moraes, A. H. (2019). Zika virus proteins at an atomic scale: how does structural biology help us to understand and develop vaccines and drugs against Zika virus infection? *J. Venomous Anim. Toxins Including Trop. Dis.* 25. doi: 10.1590/1678-9199-jvatitd-2019-0013

Verma, A. K., Noumani, A., Yadav, A. K., and Solanki, P. R. (2023). FRET Based Biosensor: Principle applications recent advances and challenges. *Diagnostics* 13, 1375. doi: 10.3390/diagnostics13081375

Vivekananda, J., Salgado, C., and Millenbaugh, N. J. (2014). DNA aptamers as a novel approach to neutralize *Staphylococcus aureus* α-toxin. *Biochem. Biophys. Res. Commun.* 444, 433–438. doi: 10.1016/j.bbrc.2014.01.076

Wain, J., House, D., Zafar, A., Baker, S., Nair, S., Kidgell, C., et al. (2005). Vi Antigen Expression in *Salmonella enterica* Serovar *typhi* Clinical Isolates from Pakistan. *J. Clin. Microbiol.* 43, 1158–1165. doi: 10.1128/JCM.43.3.1158-1165.2005

Wan, Q., Liu, X., and Zu, Y. (2021). Oligonucleotide aptamers for pathogen detection and infectious disease control. *Theranostics* 11, 9133–9161. doi: 10.7150/thno.61804

Wang, J. Y., and Koshland, D. E. Jr. (1978). Evidence for protein kinase activities in the prokaryote Salmonella typhimurium. *J. Biol. Chem.* 253 (21), 7605–7608.

Wang, L., Wang, R., Chen, F., Jiang, T., Wang, H., Slavik, M., et al. (2017a). QCM-based aptamer selection and detection of Salmonella typhimurium. *Food Chem.* 221, 776–782. doi: 10.1016/j.foodchem.2016.11.104

Wang, R., Wang, L., Callaway, Z. T., Lu, H., Huang, T. J., and Li, Y. (2017b). A nanowell-based QCM aptasensor for rapid and sensitive detection of avian influenza virus. *Sensors Actuators B: Chem* 240, 934–940. doi: 10.1038/nature13027

Weerathunge, P., Ramanathan, R., Torok, V. A., Hodgson, K., Xu, Y., Goodacre, R., et al. (2019). Ultrasensitive colorimetric detection of murine norovirus using nanozyme aptasensor. *Analytical Chem.* 91, 3270–3276. doi: 10.1021/acs.analchem.8b03300

Weis, M., and Maisner, A. (2015). Nipah virus fusion protein: Importance of the cytoplasmic tail for endosomal trafficking and bioactivity. *Eur. J. Cell Biol.* 94, 316–322. doi: 10.1016/j.ejcb.2015.05.005

Wei-Wen Hsiao, W., Sharma, N., Le, T.-N., Cheng, Y.-Y., Lee, C.-C., Vo, D.-T., et al. (2022). Fluorescent nanodiamond-based spin-enhanced lateral flow immunoassay for detection of SARS-CoV-2 nucleocapsid protein and spike protein from different variants. *Analytica Chimica Acta* 1230, 340389. doi: 10.1016/j.aca.2022.340389

Weng, X., and Neethirajan, S. (2017). Aptamer-based fluorometric determination of norovirus using a paper-based microfluidic device. *Microchimica Acta* 184, 4545–4552. doi: 10.1007/s00604-017-2467-x

Winter, S. E., Winter, M. G., Thiennimitr, P., Gerriets, V. A., Nuccio, S. P., Rüssmann, H., et al. (2009). The TviA auxiliary protein renders the *Salmonella enterica* serotype Typhi RcsB regulon responsive to changes in osmolarity. *Mol. Microbiol.* 74, 175–193. doi: 10.1111/j.1365-2958.2009.06859.x

Xi, Z., Gong, Q., Wang, C., and Zheng, B. (2018). Highly sensitive chemiluminescent aptasensor for detecting HBV infection based on rapid magnetic separation and double-functionalized gold nanoparticles. *Sci. Rep.* 8, 9444. doi: 10.1038/s41598-018-27792-5

Xie, X., Huang, W., Shen, G., Yu, H., and Wang, L. (2022). Selection and colorimetric application of ssDNA aptamers against metamitron based on magnetic bead-SELEX. *Analytical Methods* 14, 3021–3032. doi: 10.1039/D2AY00566B

Yang, J., and Bowser, M. T. (2013). Capillary Electrophoresis–SELEX selection of catalytic dna aptamers for a small-molecule porphyrin target. *Analytical Chem.* 85, 1525–1530. doi: 10.1021/ac302721j

Yang, M., Peng, Z., Ning, Y., Chen, Y., Zhou, Q., and Deng, L. (2013). Highly specific and cost-efficient detection of *salmonella paratyphi* A combining aptamers with single-walled carbon nanotubes. *Sensors* 13, 6865–6881. doi: 10.3390/s130506865

Ye, Y., Qi, X., Wang, H., Zhao, B., Xu, L., Zhang, Y., et al. (2022). A surface-enhanced Raman scattering aptasensor for *Escherichia coli* detection based on high-performance 3D substrate and hot spot effect. *Analytica Chimica Acta* 1221, 340141. doi: 10.1016/j.aca.2022.340141

Yeom, J. H., Lee, B., Kim, D., Lee, J. K., Kim, S., Bae, J., et al. (2016). Gold nanoparticle-DNA aptamer conjugate-assisted delivery of antimicrobial peptide effectively eliminates intracellular *Salmonella enterica* serovar *typhimurium*. *Biomaterials* 104, 43–51. doi: 10.1016/j.biomaterials.2016.07.009

Yu, X., Chen, F., Wang, R., and Li, Y. (2018). Whole-bacterium SELEX of DNA aptamers for rapid detection of *E.coli* O157:H7 using a QCM sensor. *J. Biotechnol.* 266, 39–49. doi: 10.1016/j.jbiotec.2017.12.011

Yuan, B., Peng, Q., Cheng, J., Wang, M., Zhong, J., Qi, J., et al. (2022). Structure of the Ebola virus polymerase complex. *Nature* 610, 394–401. doi: 10.1038/s41586-022-05271-2

Yüce, M., Ullah, N., and Budak, H. (2015). Trends in aptamer selection methods and applications. *Analyst* 140, 5379–5399. doi: 10.1039/C5AN00954E

Zavyalova, E., Samoylenkova, N., Revishchin, A., Turashev, A., Gordeychuk, I., Golovin, A., et al. (2017). The evaluation of pharmacodynamics and pharmacokinetics of anti-thrombin DNA aptamer RA-36. *Front. Pharmacol.* 8. doi: 10.3389/fphar.2017.00922

Zhan, Z., Li, H., Liu, J., Xie, G., Xiao, F., Wu, X., et al. (2020). A competitive enzyme linked aptasensor with rolling circle amplification (ELARCA) assay for colorimetric detection of *Listeria monocytogenes*. *Food Control* 107, 106806. doi: 10.1016/j.foodcont.2019.106806

Zhang, A. P. P., Abelson, D. M., Bornholdt, Z. A., Liu, T., Woods, J. V. L., and Saphire, E. O. (2012). The ebolavirus VP24 interferon antagonist. *Virulence* 3, 440–445. doi: 10.4161/viru.21302

Zhang, X., Khan, I. M., Ji, H., Wang, Z., Tian, H., Cao, W., et al. (2020). A label-free fluorescent aptasensor for detection of staphylococcal enterotoxin a based on aptamer-functionalized silver nanoclusters. *Polymers* 12, 152. doi: 10.3390/polym12010152

Zhang, L. F., Lepenies, B., Nakamae, S., Young, B. M., Santos, R. L., Raffatellu, M., et al. (2022). The Vi Capsular polysaccharide of *Salmonella typhi* promotes macrophage phagocytosis by binding the human C-type lectin DC-SIGN. *MBio* 13 (6). doi: 10.1128/mbio.02733-22

Zhang, T., Lu, Y., Deng, S., and Deng, R. (2021). "Aptamers for the diagnosis of infectious diseases," in *Aptamers for Medical Applications* (Springer, Singapore), 207–238. doi: 10.1007/978-981-33-4838-7_8

Zhang, Y., Zhang, Y., Yang, Y., Wang, L., and Weng, L. (2013). Identification of a Pseudomonas sp. that inhibits rhl system of quorum sensing. *Indian J. Microbiol.* 53, 28–35. doi: 10.1007/s12088-012-0340-5

Zhao, Q., Du, P., Wang, X., Huang, M., Sun, L.-D., Wang, T., et al. (2021). Upconversion fluorescence resonance energy transfer aptasensors for H5N1 influenza virus detection. *ACS Omega* 6, 15236–15245. doi: 10.1021/acsomega.1c01491

Zhao, M., Li, W., Liu, K., Li, H., and Lan, X. (2019). C4-HSL aptamers for blocking qurom sensing and inhibiting biofilm formation in *Pseudomonas aeruginosa* and its structure prediction and analysis. *PLoS One* 14, e0212041. doi: 10.1371/journal.pone.0212041

Zheng, J., Tang, X., Wu, R., Yan, Q., Tang, H., Luo, J., et al. (2015). Identification and characteristics of aptamers against inactivated *Vibrio alginolyticus*. *LWT - Food Sci. Technol.* 64, 1138–1142. doi: 10.1016/j.lwt.2015.07.021

Zhou, S., Lu, C., Li, Y., Xue, L., Zhao, C., Tian, G., et al. (2020). Gold nanobones enhanced ultrasensitive surface-enhanced raman scattering aptasensor for detecting *Escherichia coli* o157:h7. *ACS Sensors* 5, 588–596. doi: 10.1021/acssensors.9b02600

Zhou, J., and Rossi, J. (2017). Aptamers as targeted therapeutics: current potential and challenges. *Nat. Rev. Drug Discovery* 16, 181–202. doi: 10.1038/nrd.2016.199

Zhou, Y., Xiong, H., Chen, R., Wan, L., Kong, Y., Rao, J., et al. (2021). Aptamer detection of *Mycobaterium tuberculosis* mannose-capped lipoarabinomannan in lesion tissues for tuberculosis diagnosis. *Front. Cell. Infection Microbiol.* 11, 634915. doi: 10.3389/fcimb.2021.634915

Zhu, L., Gao, T., Huang, Y., Jin, J., Wang, D., Zhang, L., et al. (2022). Ebola virus VP35 hijacks the PKA-CREB1 pathway for replication and pathogenesis by AKIP1 association. *Nat. Commun.* 13 (1), 2256. doi: 10.1038/s41467-022-29948-4

Zhu, C., Li, L., Yang, G., and Qu, F. (2021). Investigating the influences of random-region length on aptamer selection efficiency based on capillary electrophoresis–SELEX and high-throughput sequencing. *Analytical Chem.* 93, 17030–17035. doi: 10.1021/acs.analchem.1c03661

Zhu, S., Watanabe, M., Kirkpatrick, E., Murray, A. B., Sok, R., and Karst, S. M. (2016). Regulation of norovirus virulence by the VP1 protruding domain correlates with B Cell infection efficiency. *J. Virol.* 90, 2858–2867. doi: 10.1128/jvi.02880-15

Zou, Y., Duan, N., Wu, S., Shen, M., and & Wang, Z. (2018). Selection, identification, and binding mechanism studies of an ssdna aptamer targeted to different stages of *E. coli* O157:H7. *J. Agric. Food Chem.* 66, 5677–5682. doi: 10.1021/acs.jafc.8b01006

Zou, J., Huang, X., Wu, L., Chen, G., Dong, J., Cui, X., et al. (2015). Selection of intracellularly functional RNA mimics of green fluorescent protein using fluorescence-activated cell sorting. *J. Mol. Evol.* 81, 172–178. doi: 10.1007/s00239-015-9718-4

Zou, X., Wu, J., Gu, J., Shen, L., and Mao, L. (2019). Application of aptamers in virus detection and antiviral therapy. *Front. Microbiol.* 10, 1462. doi: 10.3389/fmicb.2019.01462

Zou, Z., Younas, T., Dumsday, G., Haritos, V. S., and He, L. (2023). Rapid production of multimeric RNA aptamers stabilized by a designed pseudo-circular structure in *E. coli*. *Biotechnol. J.* 18 (3). doi: 10.1002/biot.202200390